

Multi Scalable Design and Performance Characterization of Glass
Fiber Reinforced Epoxy Composites by Incorporation of Hexagonal
Boron Nitride in Resin and on Interfaces

by

Samet ÖZYİĞİT

Submitted to the Graduate School of Engineering and Natural Sciences

in partial fulfillment of

the requirements for the degree of

Master of Science

Sabancı University

July 2022

Multi Scalable Design and Performance Characterization of Glass
Fiber Reinforced Epoxy Composites by Incorporation of Hexagonal
Boron Nitride in Resin and on Interfaces

Approved by:

Assoc. Prof. Dr. Burcu SANER OKAN
(Thesis Supervisor)

Prof. Dr. Mehmet YILDIZ

Assoc. Prof. Dr. Bertan BEYLERGIL

Approval Date: July 26, 2022

Samet ÖZYİĞİT 2022 ©

All Rights Reserved

ABSTRACT

Multi Scalable Design and Performance Characterization of Glass Fiber Reinforced Epoxy Composites by Incorporation of Hexagonal Boron Nitride in Resin and on Interfaces

Samet ÖZYİĞİT

MATERIAL SCIENCE AND NANOENGINEERING, MASTER THESIS

JULY 2022

Thesis Supervisor: Assoc. Prof. Dr. Burcu SANER OKAN

Keywords: Hexagonal boron nitride, epoxy composites, glass fiber, thermal conductivity, mechanical properties

Thermal conductive materials are widely utilized to efficiently dissipate energy especially in the heat-generated electronic systems in aerospace systems. Polymeric materials are selected as structural materials due to their high chemical resistance, mechanical strength, and lightweight; on the other hand, their usage is restricted by their low thermal conductive nature. The particulate filler reinforcements are a promising way to enhance the thermal conductivity of the polymers since these fillers also improve the mechanical properties and preserve the structural consistency of polymers. In this thesis, epoxy is one of the most common thermoset polymers, and the incorporation of micron- and nano-sized hexagonal boron nitride (h-BN) particles in comprehensive weight percentages were performed to evaluate the effect of particle size and loading ratio on thermal conductivity enhancement of epoxy. Firstly, the micron-sized h-BN particles were integrated homogeneously into epoxy to evaluate the effect of the concentration of the h-

BN particles on the thermal and mechanical performance of the epoxy by sonication. The thermal performance of the epoxy showed significant enhancement by increasing the concentration of the h-BN particles up to 20 wt%, and the in-plane and through-thickness thermal conductivities of h-BN integrated reinforced epoxy composites improved by 107% and 112%, respectively. On the other hand, the mechanical properties exhibited an upward trend until they reached optimum concentration level, whereby tensile and flexural modulus were improved by 46.9% and 40.6% with the loading h-BN ratios of 20 wt% and 10 wt%, respectively. As a second parameter, the particle size was investigated to determine its effect on the thermal and mechanical properties by incorporation of the nano-sized h-BN in epoxy with the same loading levels. The thermal conductivity performance of the epoxy reached the highest value for 20 wt% h-BN particles with 40.5% and 35.1% enhancement levels in in-plane and through-thickness directions less than the micron-sized h-BN particles reinforced epoxy. In addition, the highest tensile and flexural modulus enhancements were achieved by 16% and 15% by incorporating 20 wt% nano-sized h-BN particles. In the second part of the study, the 10 wt% h-BN particles were integrated into neat and SWCNT coated glass fiber reinforced epoxy composites to enhance the thermal performance of the composites by vacuum infusion method, and a 32% improvement was obtained for the hybrid fabric design having neat and nano-coated fabrics together. In conclusion, the incorporation of h-BN particles with large particle sizes is an efficient way to improve the thermal performance of composite materials due to the construction of thick and stable thermal conductive pathways and the limitation of interfacial phonon scattering areas. The investigation of the particle size-concentration relationship of particulate reinforcements allows new insight in polymer matrix composites to control the thermal management in the structural application and will be a guideway for the development of new designs and multifunctional and multi-scale composites with tailored functionalities.

ÖZET

Cam Elyaf Takviyeli Epoksi Kompozitlerin Reçine ve Arayüzelere Hegzagonal Bor Nitrür Dahil Edilmesi ile Çok Ölçeklenebilir Tasarımı ve Performans Karakterizasyonu

Samet ÖZYİĞİT

MALZEME BİLİMİ VE NANOMÜHENDİSLİĞİ, YÜKSEK LİSANS TEZİ,
TEMMUZ 2022

Tez Danışmanı: Doc. Dr. Burcu SANER OKAN

Anahtar kelimeler: hegzagonal bor nitrür, epoksi kompozit, cam fiber, ısıl iletkenlik,
mekanik özellikler

Isıl iletkenlik katsayısı özellikle havacılık alanında ısı açığa çıkaran elektronik sistemlerin çevrelerinde etkin ısı dağıtımını sağlanması açısından oldukça önem taşımaktadır. Polimer malzemeler yüksek kimyasal direnç, mekanik dayanım ve hafiflik gibi özelliklerinde ötürü havacılık sistemlerinde oldukça geniş bir yer bulurken; ısıl iletim katsayılarının düşüklüğü kullanım alanını kısıtlamaktadır. Termal iletken partiküllerin kullanımını aynı zamanda yüksek mekanik performans ve yapısal süreklilik sağlamalarından dolayı polimerlerin ısıl iletkenliklerini artırmak için etkin bir yöntemdir. Bu çalışmada havacılık alanındaki en yaygın kullanıma sahip termoset polimerlerden olan epoksinin ısıl iletim katsayısının hegzagonal bor nitrür kullanılarak artırılması amaçlanmıştır. Öncelikle hegzagonal bor nitrürün konsantrasyon seviyesinin epoksinin ısıl iletkenlik ve mekanik özelliklerine etkisini incelemek amacıyla mikron boyutta h-BN partikülleri epoksi içerisine sonikasyon vasıtasıyla homojen bir şekilde dağıtılmıştır. Isıl özellikler h-BN

miktarı ile doğru orantılı olarak gelişme gösterirken; mekanik özelliklerde optimum konsantrasyon seviyesinden sonra düşüş gözlenmektedir. En yüksek düzlem içi ve kalınlık boyunca ısı iletkenlik değeri sırasıyla %107 ve %112 oranlarında artış göstermiştir. Bunun yanısıra, epoksi içerisine %20 h-BN eklenmesiyle çekme modülü değeri %46.9'luk artış elde edilirken, %10 h-BN eğme modülünü %46.9 oranında geliştirmiştir. Ayrıca, partikül boyutunun ısı ve mekanik özelliklere etkisini kıyaslamak amacıyla mikron boyutta h-BN partikülleri ile aynı oranlarda nano boyutta h-BN partikülleri epoksi içerisine entegre edilmiştir. ısı iletkenlik değeri partikül miktarıyla artış göstermektedir ve düzlem içi ve kalınlık boyunca maksimum artış sırasıyla %40.5 ve %35.1 olarak elde edilmiştir ki bu oranlar mikron boyutta h-BN'nin yarısından daha düşük değerlerdedir. Ayrıca, çekme ve eğme modüllerinde de %16 ve %15 oranlarında artış mevcuttur. Çalışmanın ikinci bölümünde ağırlıkça %10 oranında mikron boyutlu h-BN partikülleri tek duvarlı karbon nanotüp kaplı cam fiber takviyeli kompozitlere vakum infüzyon metodu yardımıyla entegre edilmiştir. Karbon nanotüpler epoksi ile cam fiberler arasındaki termal uyumsuzluğu giderirken; %10 h-BN eklenmesiyle de termal iletkenlikte %32 artış gözlemlenmiştir. Sonuç olarak, yüksek partikül boyutuna sahip h-BN partikülleri kompozit malzemelerin termal performanslarını geliştirmede geniş ve kararlı ısı iletim yolunun oluşumu ve ısı saçılmaya neden olan arayüzey miktarının azalması nedeniyle etkin bir yaklaşımdır. Ayrıca bu çalışmada, partikül takviyelerin partikül boyu- konsantrasyon ilişkisi araştırılarak polimer matris kompozitlerin ısı yönetim amacıyla yapısal alanlarda üretimlerine yeni bir bakış açısı kazandırılmış olup bu çalışma kompozit malzemelerin fonksiyonel yeni tasarımları için bir rehber oluşturacaktır.

ACKNOWLEDGEMENTS

I feel so lucky considering that there is a huge family behind this thesis without whom it might not have been completed. First of all, I would like to express my profound gratitude to my supervisor, Assoc. Prof. Dr. Burcu Saner Okan, for her valuable guidance and constructive feedback throughout the process. Imbued with her critical approach, I understand at the very beginning of my career that there is always room for improvement, which obviously motivates me to work harder and smarter.

I would like to extend my thanks to Prof. Dr. Mehmet Yıldız whose meaningful presence at each step of the process paved the way for further encouragement and improvement. Also, I would like to give my sincere thanks to Assoc. Prof. Dr. Bertan Beylergil for his support in composite manufacturing and characterization.

I would like to thank to my colleague Kuray Dericiler for SEM characterization, Dr. Semih Doğan for his help in XPS characterization and his support in Wet Chemistry Laboratory of SUIMC. Also, SUIMC's technicians of Feyyaz Perem, Sezer Özdemir and Sinan Ayazlı support me to carry out experiments in the laboratory. I would like to thank to Isa Emami Tabrizi and Abdulrahman Al-Nadhari for composite manufacturing and their continuous support.

This process was not always smooth sailing; however, it was absolutely more bearable thanks to my friends. As such, I would like to express my sincere gratitude to Sinem Elmas, Nihan Birgün, Mostafa Mehdipour Aghbolagh, Sercan Akgün, Orhun Şenol, Fethiye Esin Yakın, Sina Khalilvandi Behrouzgar, Nargiz Aliyeva, Atakan Koçanalı, and especially to Esra Yalçınkaya for always going above and beyond as friends.

I wish to express my deep gratitude to my family, who has always been the wind beneath my wings, for the unwavering support and endless sacrifices that have afforded me this opportunity.

Lastly, but most importantly, I would also like to gratefully acknowledge the Turkish Energy Nuclear and Mineral Research Agency-National Boron Research Institute (TENMAK-BOREN) for the financial support to the project numbered 2020-31-07-15-002, and the Scientific and Technical Research Council of Turkey (TUBITAK) 1003 programme for the scholarship within the scope of the project numbered 218M709.

To my beloved family...

TABLE OF CONTENTS

ABSTRACT.....	iv
ÖZET	vi
ACKNOWLEDGEMENTS.....	viii
LIST OF TABLES.....	xii
LIST OF FIGURES	xiii
LIST OF ABBREVIATIONS.....	xv
CHAPTER 1. STATE-OF-THE-ART	1
CHAPTER 2. THE EFFECT OF PARTICLE SIZE AND LOADING RATIOS OF HEXAGONAL BORON NITRIDE (h-BN) PARTICLES ON THE THERMAL MANAGEMENT AND MECHANICAL PERFORMANCE OF EPOXY COMPOSITES	2
2.1. Introduction.....	2
2.2 Experimental.....	4
2.2.1 Materials.....	4
2.2.2 Fabrication of micron- and nano-sized h-BN reinforced epoxy composites	5
2.2.3 Characterization	6
2.3. Results & Discussion.....	7
2.3.1. The characteristic properties of micron- and nano-sized h-BN reinforcements	7
2.3.2. The effect of particle size and loading ratios of h-BN particles on the mechanical and thermomechanical performance of epoxy composites	10
2.3.3. Tailored thermal conductivity of epoxy composites as a function of particle size and loading ratio of h-BN particles.....	18
2.3.4. Fracture surface analysis of neat and h-BN reinforced epoxy composites in terms of micron- and nano-sized h-BN particles	21
2.4. Conclusion	24

CHAPTER 3. THE SYNERGISTIC EFFECT OF CARBON NANOMATERIAL COATED GLASS FIBERS ON THE PERFORMANCE OF EPOXY COMPOSITES HAVING h-BN PARTICLES	26
3.1. Experimental.....	26
3.1.1. Materials.....	26
3.1.2. The selective dispersion of micron-sized h-BN and SWCNT in resin and fiber interfaces	27
3.1.3. Preparation of Composites having different designs by Vacuum Infusion and Hand Lay-up combined with Hot Press Methods	27
3.1.4. Characterization	29
3.2. Results & Discussion	30
3.2.1. The characteristic properties of neat and SWCNT coated glass fabrics	30
3.2.2. The characteristic properties of composites having different designs	35
3.2.3. The effect of the h-BN and SWCNT on the mechanical and thermomechanical properties of composites having different designs in resin and interface	38
3.2.4. Tailored thermal conductivity of composites as a function of h-BN incorporation in resin and SWCNT coating in interface	46
3.3 Conclusion	49
CHAPTER 4. CONCLUSION	51
REFERENCES	53

LIST OF TABLES

Table 1. The elemental compositions of micron- and nano-sized h-BN particles	8
Table 2. Tensile strength and modulus values and their improvement percentages of micron-sized h-BN reinforced epoxy composites as a function of loading ratio	12
Table 3. Tensile strength and modulus values and their improvement percentages of nano-sized h-BN reinforced epoxy composites as a function of loading ratio	13
Table 4. Flexural modulus and strength values and their improvements of micron-sized h-BN particles reinforced epoxy composites as a function of loading ratio.....	15
Table 5. Flexural modulus and strength values and their improvements of nano-sized h-BN particles reinforced epoxy composites as a function of loading ratio	16
Table 6. The thermal conductivity of micron-sized h-BN reinforced epoxy composites in in-plane and through-thickness directions as a function of loading ratio	20
Table 7. The thermal conductivity of nano-sized h-BN reinforced epoxy composites in in-plane and through-thickness directions as a function of loading ratio	21
Table 8. The density values of the composite materials having different designs.....	37
Table 9. Tensile strength, modulus, and strain values and their improvement percentages of the glass fiber reinforced composites as a function of usage of the h-BN and SWCNT in resin and interfaces	40
Table 10. The thermal conductivity values and their improvements of the glass fiber reinforced composites with different designs in in-plane and through-thickness directions as a function of h-BN and SWCNT in resin and interfaces	47

LIST OF FIGURES

Figure 1. The schematic representation of the micron- and nano-sized h-BN reinforced epoxy composites fabrication process	6
Figure 2. SEM images of (a) micron- and (b) nano-sized h-BN particles	7
Figure 3. XPS survey scan spectra of micron- and nano-sized h-BN particles	8
Figure 4. XRD patterns of micron- and nano-sized h-BN particles	9
Figure 5. TGA curves of micron- and nano-sized h-BN particles	9
Figure 6. Raman spectra of micron- and nano-sized h-BN particles	10
Figure 7. Tensile stress-strain curves of (a) micron- and (b) nano-sized h-BN reinforced epoxy composites as a function of different loadings, and comparison of (c) tensile strength improvement and (d) tensile modulus improvement in terms of micron- and nano-sized h-BN particles.....	12
Figure 8. Flexural stress-strain curves of (a) micron- and (b) nano-sized h-BN epoxy composites as a function of different loadings, and comparison of (c) flexural strength improvement and (d) flexural modulus improvement in terms of micron- and nano-sized h-BN particles	15
Figure 9. Temperature sweep of the storage modulus of (a) micron-sized and (b) nano-sized h-BN reinforced epoxy composites, and damping ratio curves of (c) micron-sized and (d) nano-sized h-BN reinforced epoxy composites.....	18
Figure 10. The comparison of the thermal conductivity values of the epoxy composites in (a) in-plane (b) through-thickness directions as a function of particle size and concentration of h-BN particles	20
Figure 11. SEM images of the fracture surfaces after tensile test (a,b) neat epoxy (c,d) 10 wt% micron-sized h-BN reinforced epoxy composite, and (e,f) 10 wt% nano-sized h-BN reinforced epoxy composite.....	23
Figure 13. The schematic representation of the glass fiber reinforced composites production procedure by the vacuum infusion method	28
Figure 14. The schematic representation of the glass fiber reinforced composites production procedure by the hand lay-up combined with the hot press method	29
Figure 15. Optical microscopy images of glass fibers (a,b) as-received (c,d) after the SWCNT coating.....	31
Figure 16. SEM images of the glass fibers (a,b) as-received and (c,d) after the dip-coating of SWCNT	33

Figure 18. Raman spectra of SWCNT, neat and SWCNT coated glass fibers	34
Figure 19. The percentages of weight loss of micron-sized h-BN, neat glass fabric and SWCNT coated glass fabric.....	35
Figure 20. The optical microscopy images of the (a,b) neat fabric/neat resin (c,d) neat fabric/10 wt% m/h-BN epoxy resin (e,f) hybrid fabric/neat resin (g,h) hybrid fabric/10 wt% m/h-BN epoxy resin (i,j) full SWCNT coated fabric/neat resin.....	37
Figure 21. The weight loss percentage variations of the composites having different designs with temperature	38
Figure 22. (a) Tensile stress-strain curves, and (b) tensile strength and modulus improvements of the composites having different designs.....	41
Figure 23. (a) Flexural stress-strain curves (b) flexural strength and modulus improvements of the composites having different designs.....	42
Figure 24. The impact strength variations of the composites in terms of the h-BN and SWCNT utilization in resin and interfaces	44
Figure 25. (a) Temperature sweeps of the storage modulus and (b) damping ratio curves of the composite with different designs	46
Figure 26. Comparison of the in-plane and through-thickness thermal conductivity values of the composites with different designs as a function of h-BN and SWCNT particles in resin and interfaces	49

LIST OF ABBREVIATIONS

DMA	Dynamical Mechanical Analysis
DSC	Differential Scanning Calorimetry
eV	Electron Volt
FTIR	Fourier Transform Infrared Spectroscopy
h-BN	Hexagonal Boron Nitride
RAMAN	Renishaw inVia Reflex Raman Microscopy System
SEM	Scanning Electron Microscope
SWCNT	Single-Walled Carbon Nanotubes
T_g	Glass Transition Temperature
TGA	Thermogravimetric Analysis
UTM	Universal Testing Machine
VARTM	Vacuum-Assisted Resin Transfer Method
W/m.K	Watt to meter.Kelvin ratio
XPS	X-ray Photoelectron Spectroscopy
XRD	X-ray Diffraction

CHAPTER 1. STATE-OF-THE-ART

Epoxy is one of the most common thermoset polymers used for structural composites, electronic packaging, adhesive, and coatings in electronics due to its high chemical resistance, stability, mechanical properties, and processability [1]. However, epoxy exhibits a thermal insulator property in which thermal conductivity is in the range of 0.1-0.5 W/m.K like other types of polymer, and this inherent property limits the usage of the epoxy in the heat-generated areas [2].

The incorporation of the thermal conductive fillers is an effective and economical way to enhance the thermal performance of the epoxy [3]. Furthermore, there are two types of inorganic fillers which is commonly utilized to improve the thermal conductivity of the polymers. The first group consists of fillers with electrical conductivity such as carbon nanotubes (CNT), gold, copper, and silver [4]. These fillers improve the thermal conductivity of the composites; on the other hand, the electrical insulation property deteriorated, which limits the usage of the final composites in specific areas that need electrical insulation properties. In the second group, the usage of ceramic-based fillers is the alternative way to increase the thermal conductivity of polymers, whereas the electrical insulation property is preserved [5].

h-BN particles are promising candidates with high in-plane conductivity values of 550W/m.K and electrical insulator properties with a band gap between 5.5 to 6.4 eV. Additionally, the outstanding mechanical strength and excellent chemical inertness provide a wide variety of application areas such as thermally conductivity nanocomposites, electrocatalysts, field emitters, and so on [6][7].

In the current study, h-BN particles as resin and interface modifiers were utilized to fabricate multi-scale composites with excellent thermal performance supported by high mechanical and thermomechanical properties. In the first part of the study, the micron- and nano-sized h-BN particles with a comprehensive loading ratio are incorporated into resin to evaluate the effect of particle size and concentration on the thermal and mechanical properties of epoxy. In the second part, h-BN particles in the optimum loading level and single walled carbon nanotubes (SWCNT) are utilized to observe the synergistic effects of micron- and nano-sized filler on the glass fiber reinforced epoxy composites.

CHAPTER 2. THE EFFECT OF PARTICLE SIZE AND LOADING RATIOS OF HEXAGONAL BORON NITRIDE (h-BN) PARTICLES ON THE THERMAL MANAGEMENT AND MECHANICAL PERFORMANCE OF EPOXY COMPOSITES

Micron- and nano-sized h-BN particles are incorporated in epoxy for manufacturing high thermal conductive composites in a comprehensive weight ratio to determine the effects of particle size and loading ratio on thermal and mechanical performance. In the investigation of the loading ratio effects as a first parameter, the pre-dispersion method is employed for the selective dispersion of micron-sized h-BN particles with a weight ratio from 0.5 wt% to 20 wt% in epoxy. The homogeneous and stable dispersion of h-BN particles enhances the thermal and mechanical performance through efficient heat dissipation and load transfer. In the second approach, the nano-sized h-BN particles in the same loading ratios are dispersed in epoxy to evaluate the particle size effects on the properties of epoxy. The synergetic effects of particle size and loading ratios of h-BN particles are determined in detail by utilizing thermal characterization techniques supported by mechanical and thermomechanical methods. The h-BN reinforced epoxy composites show improved thermal and mechanical performance with increasing particle size and loading ratio. In the micron-sized h-BN reinforced epoxy, promising enhancements are observed in thermal conductivity in in-plane and through-thickness directions by 107% and 112% for 20 wt% loading level, respectively, and remarkable improvements in tensile modulus by 41% as well as flexural modulus by 42% for 10 wt% h-BN concentration.

2.1. Introduction

Polymer composites are being extensively used in the aerospace industry since they offer significant weight reduction, higher fatigue, and corrosion resistance over the traditional metallic counterparts. However, polymers have a poor thermal conductivity in the range of 0.1–0.5 W/m.K due to the random orientation of molecular chains or the defects like a loop, voids, impurities, and chain dangling ends. These defects give rise to phonon scattering and considerable reduction in phonon's mean free path, thereby decreasing the thermal conductivity, which causes the failure of polymer composites when the temperature increases [8][9]. At this point, complex and high-powered electronics components and systems used on modern aircraft generate large amounts of waste heat.

For instance, the peak thermal load of the equipment cabin in the F-22 can reach up to 50 kW, and the total thermal load of the entire F-22 can exceed 100 kW [10]. The waste heat coming from the onboard electronics, oil and hydraulic systems, avionics bay cooling, and weapons modules must be dissipated efficiently to ensure thermal stability and prevent material failure, in other words, to maintain safe and reliable operation. Therefore, thermal conductivity should be tailored gradually, and the development of thermally conductive high-performance polymer composites that can control heat dissipation is of paramount importance in aerospace applications [11][12].

There are two ways to enhance the thermal conductivity of polymers: (i) molecular engineering of polymer chains and (ii) blending polymers with high thermal conductive metallic or ceramic micron- and nano-sized particles. Considering long-term costs, process complexity, and structural performance, the latter is much more efficient in enhancing the thermal conductivity of a polymer. As the amount of filler is adequate, 3D thermally conductive networks are formed inside the polymer, which facilitates thermal conductivity improvement. Therefore, most of the studies have been reported employing different kinds of fillers like metallic [13], ceramic [14][15], natural[16][17], and carbon [18][19] fillers in thermoset and thermoplastic composites. Metallic and carbon fillers increase the electric conductivity among these fillers, which is not appropriate for specific applications like wearable electronic gadgets, food industries, and electrical contacts. However, ceramic-based fillers have an advantage that only improves the thermal conductivity and keeps the electrical insulation of polymers [5][20]. At this point, hexagonal boron nitride (h-BN) is a promising thermally conductive dielectric material for thermal management systems since its theoretical in-plane thermal conductivity is reported as 550 W/m.K at room temperature [7]. In the literature, there are several attempts to investigate the thermal, mechanical, and thermomechanical properties of epoxy composites by incorporating h-BN particles at different loadings. The important point which should be considered in the addition of fillers is the effect of the loading ratio of fillers to epoxy. For instance, Gu et al. [21] investigated the effects of the loading ratio of neat and modified micron-sized BN particles on thermal and mechanical properties, and the maximum thermal conductivity and flexural strength exhibited 58% and 13% improvement at 10 wt% neat BN concentration, respectively. In addition, Tang et al. [22] works on the concentration of h-BN on epoxy, and the thermal conductivity value of epoxy is enhanced by 58% for a 7 wt% h-BN loading level. On the other hand, Hou et al.

[2] pointed out that the thermal conductivity value reaches maximum improvement by 235% with an addition of 30 wt% h-BN, as well as 0.5 wt% of h-BN particles improve the mechanical properties by 5.7%. Up to now, there are numerous works for the enhancement of thermal conductivity of epoxy composites; however, there is no systematics for the selection of an ideal h-BN filler to enhance through-thickness and in-plane thermal conductivity. At high loading ratios, it is possible to get high thermal conductivity, but there is a drastic decrease in mechanical properties. Herein, it is significant to tailor the particle size of h-BN and investigate the particle size effect by decreasing the filler amount and addressing interfacial areas. To the best of our knowledge, there is no work that addresses the selection of h-BN particles with an ideal particle size and optimum concentration level to tailor through-thickness and in-plane thermal conductivity.

In the present work, the ethanol-assisted pre-dispersion method was utilized to incorporate micron- and nano-sized h-BN particles in epoxy to modify thermal and mechanical properties without the deterioration of the inherent properties of the resin. This technique is fast, up-scalable, and cost-effective because the solvent-based method decreases the viscosity of the epoxy and provides efficient dispersion media for h-BN particles. In the first step of the work, micron- and nano-sized h-BN with a comprehensive weight range were selectively dispersed in epoxy to evaluate the effect of the particle size on the thermal and mechanical properties of the epoxy; subsequently, final mixtures were utilized to produce the epoxy composites by applying a classical molding method. With this study, it becomes possible to understand the effect of the particle size distribution of h-BN particles on through-thickness and in-plane thermal conductivity of glass fiber reinforced epoxy composites with a comprehensive mechanical and thermomechanical characterization.

2.2 Experimental

2.2.1 Materials

Hexagonal boron nitride (h-BN) with the particle size of 120 nm was purchased from Bortek Company from Turkey. h-BN with the particle size changing 4-10 μm was obtained from Civelek Porselen Company from Turkey. A high T_g thermosetting resin system, Sika Biresin® CR131 (based on 50%–100% bisphenol A diglycidyl ether (DGEBA), 10%–20% bisphenol F diglycidyl ether (DGEBF), and 5%–10% 1,4-bis (2,3 epoxypropoxy) butane) with CH132-5 hardener (based on triethylenetetramine [TETA]),

were supplied by Tekno Chemicals Inc., Turkey. This resin system is suitable for infusion applications due to its low viscosity and is generally used to manufacture high-performance fiber-reinforced composites parts. Also, the ethanol (99%) was purchased from Sigma Aldrich. All agents were used in their analytical grades without any treatment.

2.2.2 Fabrication of micron- and nano-sized h-BN reinforced epoxy composites

To produce the reference epoxy plates, the CR131 epoxy was mixed with the CH132-5 hardener in the proper mix ratio (100:28 by weight- in accordance with manufacturer's data) using a high-speed shear mixer (Thinky-mixer) for 1 min at 1000 rpm. After mixing, the resin was degassed in a vacuum chamber for 25 min to eliminate all voids in the prepared solution. Then, it was poured into a preheated aluminum mold and cured at 100 °C for 5 h in an oven. The pre-dispersion method was used to produce the well-dispersed h-BN reinforced epoxy composite plates with a wide weight percentage range from 0.5 wt% to 20 wt% by means of probe sonicator (Hielscher UP400S) at room temperature. The micron- and nano-sized h-BN particles were probe-sonicated in ethanol for 1 h, and then the h-BN/ethanol mixture was added to the epoxy and sonicated for an additional 2 h. All sonication processes were carried out in an ice bath to inhibit the heating of the solution. The homogenous h-BN/ethanol/epoxy solution was stirred using a magnetic stirrer for 2 days to remove all ethanol in the mixture. After the addition of the CH132-5 hardener and the degassing step having the same procedure as preparing a reference epoxy plate, the mixture was poured into again a preheated aluminum mold and cured at 100 °C for 5 h in an oven. Fig. 1 exhibits the schematic of the preparation process of the h-BN epoxy mixture. As a last step of production, the manufactured reference and h-BN reinforced epoxy composites were cut to the determined dimensions by ASTM and ISO standards using a CNC machine.

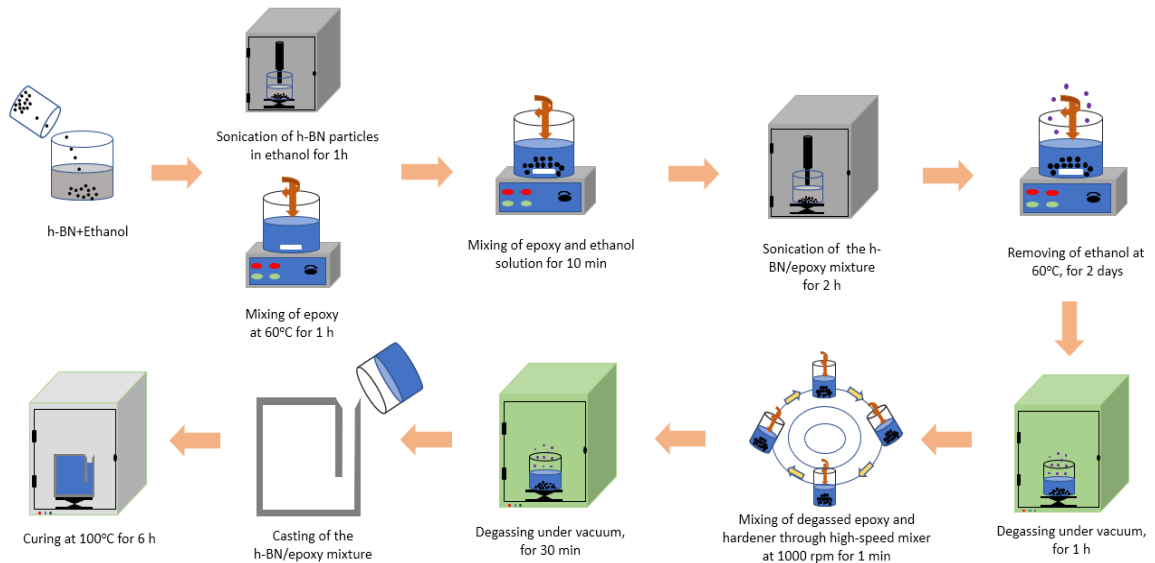


Figure 1. The schematic representation of the micron- and nano-sized h-BN reinforced epoxy composites fabrication process

2.2.3 Characterization

Various microscopic and spectroscopic characterization techniques were conducted to identify the properties of reinforcing agents and composite materials. The morphologies of neat micron- and nano-sized h-BN and fracture surface of samples after tensile test were examined by Leo Supra 35VP Field Emission Scanning Electron Microscope (SEM, Carl Zeiss AG, Jena, Germany). Raman spectroscopy was carried out to analyze the molecular structure and vibrational properties of both micron- and nano-sized h-BN particles by using a Renishaw inVia Reflex Raman Microscope with 532 nm edge laser at room temperature in the range of 100–3500 cm^{-1} . X-ray photoelectron spectroscopy (XPS, Thermo Scientific, Waltham, Massachusetts, USA) technique was utilized to obtain a chemical and elemental analysis of filler materials. X-Ray Diffraction (XRD) analysis was performed to determine the characteristic h-BN peaks, thereby crystal structure of micron- and nano-sized h-BN reinforcements by utilizing a Bruker D2 Phaser diffractometer with a $\text{CuK}\alpha$ radiation source. Thermogravimetric analysis (TGA) was conducted to investigate the thermal stability and weight loss percentage of filler materials by using Mettler Toledo Thermal Analyzer (TGA/DSC 3+) with a 3 $^{\circ}\text{C}/\text{min}$ heating rate from room temperature to 1000 $^{\circ}\text{C}$. Besides the analyzing of reinforcement particles, the mechanical tests were performed by Instron 5982 Static Universal Test Machine (UTM) with 10 kN load cells as well as a cross head speed of 2 mm/min. ASTM D 638 and ASTM D 790 test standards were utilized for tensile and 3-point bending tests,

respectively. Furthermore, a knife-edge extensometer (Epsilon, Tech. Corp.) was used to record the axial and transverse extension data during the tests. Dynamic mechanical analyzer (DMA) tests were carried out on the specimens with a dimension of 65 mm in length and 10 mm in width using a DMA Q800 (TA Instruments, New Castle, DE) in a dual cantilever mode for thermomechanical analysis with the heating rate of 3 °C/min by starting from room temperature to 150 °C and 1 Hz. Also, in-plane and through-thickness thermal conductivity values (k) of the reference and h-BN reinforced epoxy composite samples were measured by the hot disc method with the TPS 2500 S device.

2.3. Results & Discussion

2.3.1. The characteristic properties of micron- and nano-sized h-BN reinforcements

Surface chemistry and morphology have a significant role on the dispersion capability of fillers in polymer matrix, thus mechanical and thermal properties of final composite materials are affected by the surface properties of reinforcements and their interfacial interactions with the selected matrix. The atomic content and surface shape of h-BN can directly affect the dispersion behavior in the epoxy matrix. Within this work, two types of h-BN with different sizes were characterized by morphological and spectroscopic characterization. Fig. 2a and 2b shows SEM images of micron- and nano-sized h-BN particles. Flat-like h-BN particles are clearly detected in SEM images. From the particle size analysis results, the particle sizes of micron- and nano-sized h-BN are 4-10 μm and 120 nm, respectively. SEM images also confirmed the differences in the sizes of h-BN particles and the sheet size of micron-sized h-BN is comparably larger than nano-sized h-BN.

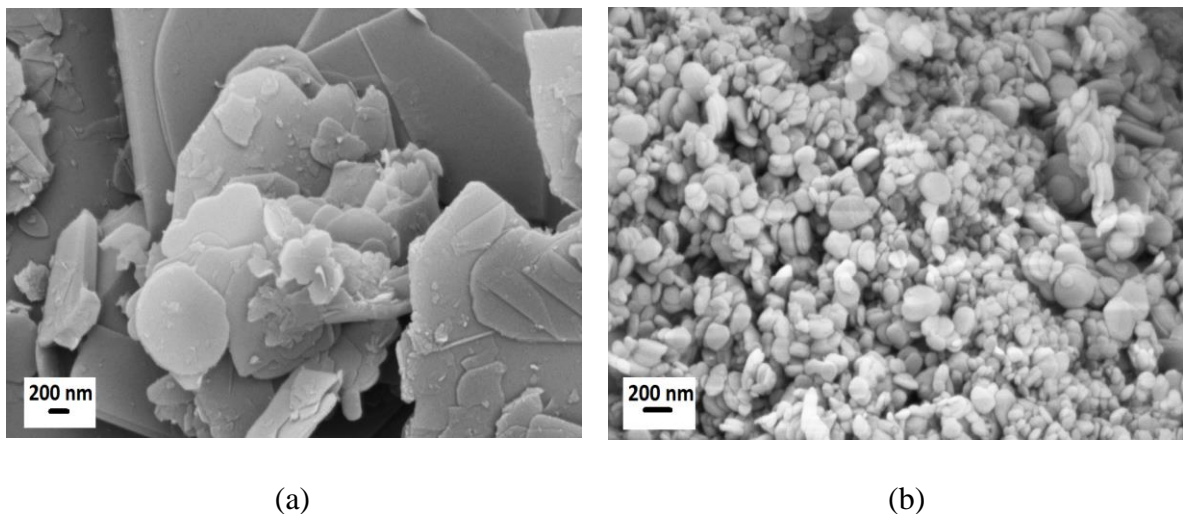


Figure 2. SEM images of (a) micron- and (b) nano-sized h-BN particles

The elemental compositions of the micron- and nano-sized h-BN particles were analyzed by XPS to understand the relation of h-BN surface chemistry with the epoxy matrix. Table 1 summarizes XPS results of neat nano- and micron-sized h-BN particles, and Fig. 3 shows XPS survey scan spectra of h-BN particles. The results indicated that nano-sized h-BN has higher oxygen and carbon contents than micron-sized h-BN. The intensity of N1s of micron-sized h-BN is higher than that of nano-sized h-BN; in addition, O1s, N1s, C1s, and B1s signals were observed at approximately 532 eV, 398 eV, 285 eV, and 190 eV, respectively, for both micron- and nano-sized h-BN, as seen in Fig. 3.

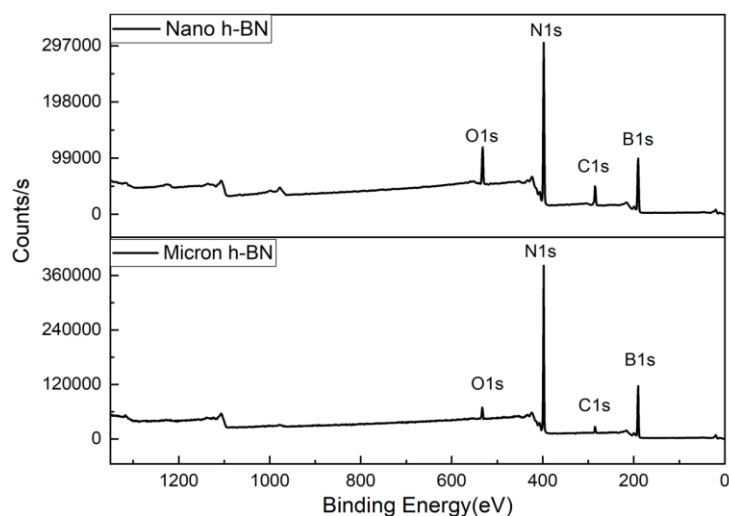


Figure 3. XPS survey scan spectra of micron- and nano-sized h-BN particles

Table 1. The elemental compositions of micron- and nano-sized h-BN particles

Sample	N (at %)	B (at %)	O (at %)	C (at %)
Micron h-BN	70.94	16.44	4.08	8.55
Nano h-BN	50.84	27.93	8.70	12.53

XRD is a non-destructive analysis method that is very useful to investigate the crystallinity and phase of the materials. Fig. 4 shows XRD patterns of micron- and nano-sized h-BN particles, and peaks found at 9°, 18°, 28°, 37°, and 48° refer to the characteristic hexagonal basal planes, (101), (102), (004), and (110), respectively.

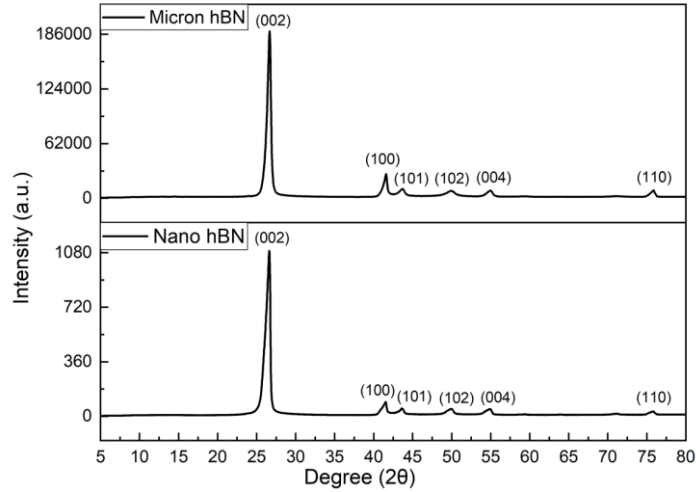


Figure 4. XRD patterns of micron- and nano-sized h-BN particles

TGA is a versatile method to investigate the thermal stability and weight loss percentage of materials. Fig. 5 exhibits the TGA curves of the neat micron- and nano-sized h-BN particles; both micron- and nano-sized h-BN particles absorb a lesser amount of moisture which is evaporated until 100 °C in their volume. Furthermore, neat and micron-sized h-BN, used for manufacturing the composite materials, were dried overnight before the utilization due to moisture absorption.

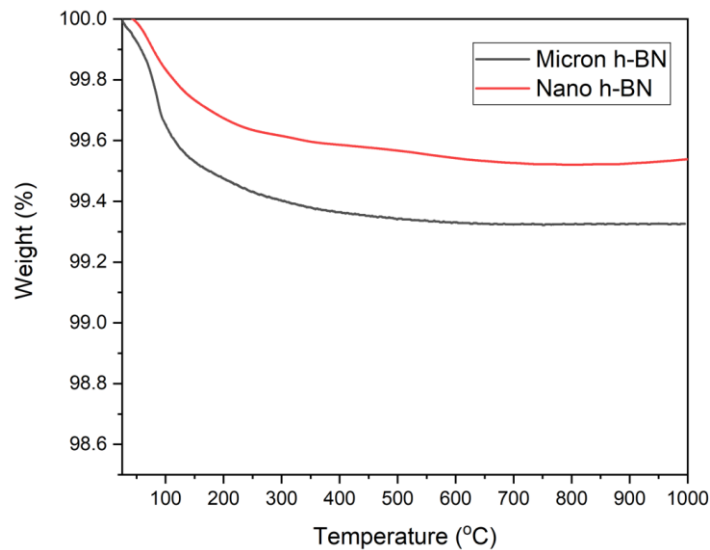


Figure 5. TGA curves of micron- and nano-sized h-BN particles

Fig. 6 exhibits the Raman spectra of micron- and nano-sized h-BN particles. The strong peak is observed at 1365 cm^{-1} in both micron- and nano-sized h-BN, and this peak is about a high-frequency interlayer Raman active E_{2g} mode. The differences in intensity of the peak can be explained by the variation of chemical bonds.

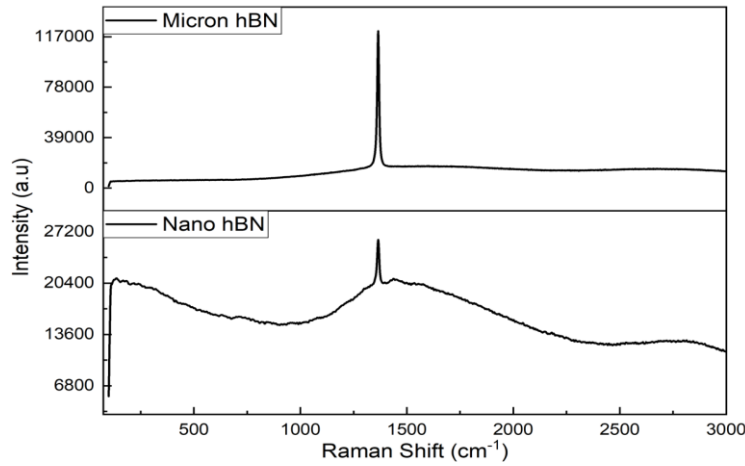


Figure 6. Raman spectra of micron- and nano-sized h-BN particles

2.3.2. The effect of particle size and loading ratios of h-BN particles on the mechanical and thermomechanical performance of epoxy composites

The flat-like particles provide high surface area, and the particle size and aspect ratio can directly affect the mechanical performance of the epoxy since particles with large particle size and aspect ratio facilitate the effective stress transfer between epoxy and h-BN particles and polymer chain movement prevention [23]. The loading ratio is another factor that enhances the mechanical properties of epoxy through inhibition of the crack propagation and providing the effective stress transfer; on the other hand, the mechanical properties when the concentration exceeds a certain level show decrement because of the bubble and stress concentration regions formation caused by aggregation of the particles [21]. In contrast, the high dispersion quality of h-BN particles and strong adhesion between h-BN and epoxy enhance the mechanical performance of the composites by inhibiting the stress concentration areas in the material [24]. Fig. 7a and 7b represent the tensile stress-strain curves for micron- and nano-sized h-BN particles reinforced epoxy as a function of loading levels, respectively. The steep elastic deformation zone, which is an indicator of brittle behavior, is observed with increasing micron-sized h-BN concentration; however, the composites, including nano-sized h-BN particles, preserve their ductile nature. In addition, Fig. 7c and 7d exhibit the comparison of the tensile strength and elastic modulus improvement in terms of micron- and nano-sized h-BN particles, respectively. The elastic modulus values show an incremental trend after 1 wt% concentration level for both micron- and nano-sized h-BN particles, and the maximum enhancement of 46.9% is obtained in the epoxy with 20 wt% micron-sized h-BN particles, which is approximately 3 times higher than 20 wt% nano-sized particles. The

enhancement is attributed to the high aspect ratio of the micron-sized h-BN particles, which allow effective constraints of crack propagation, immobilization of epoxy chains, and stress transfer between micron-sized h-BN and epoxy through a wider surface contact area of the micron-sized h-BN [25]. In addition, Table 2 and Table 3 summarize the tensile strength variation for micron- and nano-sized h-BN particles as a function of loading level. The micron-sized h-BN significantly deteriorates the tensile strength of epoxy with the increase of the loading level, which can be caused by the non-uniform distribution of h-BN and inefficient stress transfer between h-BN and epoxy, thereby the maximum reduction is observed by 20.6% for 10 wt% h-BN levels. Furthermore, nano-sized h-BN slightly changes the mechanical performance of the epoxy because local stress areas arising from the stiffening effect of the brittle crosslinked polymers and poor connections between fillers and matrix can cause a reduction in tensile strength [3] [26].

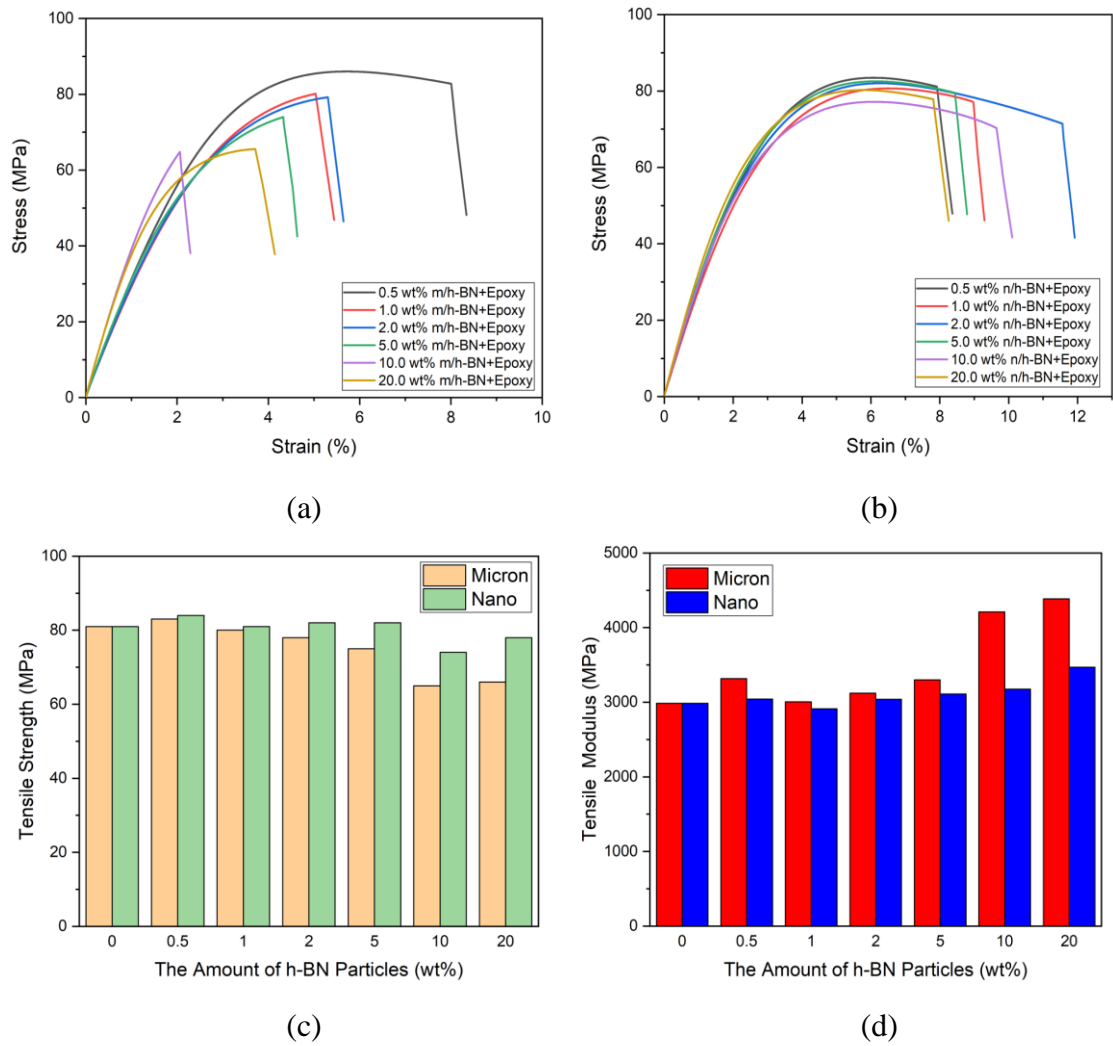


Figure 7. Tensile stress-strain curves of (a) micron- and (b) nano-sized h-BN reinforced epoxy composites as a function of different loadings, and comparison of (c) tensile strength improvement and (d) tensile modulus improvement in terms of micron- and nano-sized h-BN particles

Table 2. Tensile strength and modulus values and their improvement percentages of micron-sized h-BN reinforced epoxy composites as a function of loading ratio

Sample	Elastic Modulus (MPa)	Improvement (%)	Tensile Strength (MPa)	Improvement (%)
Neat epoxy	2985±87	-	81±2.4	-
0.5 wt% m/h-BN+Epoxy	3317±77	11.1	83±6.1	2.5
1.0 wt% m/h-BN+Epoxy	3006±49	0.7	80±0.8	-1.2
2.0 wt% m/h-BN+Epoxy	3122±29	4.6	78±2.5	-3.7

5.0 wt% m/h-BN+Epoxy	3330±33	11.6	75±2.5	-7.4
10.0 wt% m/h-BN+Epoxy	4211±90	41.1	65±5.0	-19.8
20.0 wt% m/h-BN+Epoxy	4387±83	46.9	66±0.9	-18.5

Table 3. Tensile strength and modulus values and their improvement percentages of nano-sized h-BN reinforced epoxy composites as a function of loading ratio

Sample	Elastic Modulus (MPa)	Improvement (%)	Tensile Strength (MPa)	Improvement (%)
0.5 wt% n/h-BN+Epoxy	3043±61	1.9	84±0.5	3.7
1.0 wt% n/h-BN+Epoxy	2913±23	-2.4	81±0.4	-
2.0 wt% n/h-BN+Epoxy	3039±41	1.8	82±0.2	1.2
5.0 wt% n/h-BN+Epoxy	3111±82	4.2	82±0.2	1.2
10.0 wt% n/h-BN+Epoxy	3175±53	6.4	74±7.3	-8.6
20.0 wt% n/h-BN+Epoxy	3468±30	16.2	78±6.5	-3.7

The 3-point bending test was conducted to determine the optimum particle size and loading ratio of h-BN particles to attain high performance mechanical properties of the micron- and nano-sized h-BN reinforced epoxy with high thermal conductivity values. Fig. 8a and 8b exhibit the flexural stress-strain curves for epoxy including micron- and nano-sized h-BN particles with a comprehensive weight concentration from 0.5 wt% to 20 wt%, respectively. In addition, Fig. 8c and 8d show flexural strength and modulus improvements of epoxy composites as a function of the h-BN type and its concentration. The gradual enhancement is observed in flexural modulus values for both micron- and nano-sized h-BN/epoxy composites after 1 wt% h-BN loading level; nevertheless, the flexural modulus show decrement which is owing to agglomeration of the h-BN particles when the concentration of micron-sized h-BN particles exceed the 10 wt%. The homogeneous dispersion is provided even in high concentration levels for nano-sized h-BN particles, while the 10 wt% is the upper limit for homogeneous dispersion of micron-sized h-BN particles in epoxy. Table 4 and Table 5 summarize the flexural modulus, strength, and their improvement percentages. The 10 wt% micron-sized h-BN particles

reinforced epoxy shows 40.62% improvement with respect to the neat epoxy; on the other hand, nano-sized h-BN particles enhance the flexural modulus without any aggregation in high concentrations, and the higher flexural modulus improvement percentage is 15.13% for 20 wt% loading level. The micron-sized h-BN particles enable a wider surface interaction area with epoxy, and efficient load transfer takes place between micron-sized h-BN particles and epoxy with respect to nano-sized h-BN particles; thus, the flexural modulus reaches higher values for micron-sized h-BN reinforced epoxy [27]. Otherwise, the deterioration of the flexural modulus of the micron-sized h-BN reinforced epoxy is attributed to the formation of the agglomeration of h-BN particles because agglomeration causes the formation of the stress transfer areas and reducing of the interaction areas between h-BN particles and efficient load transfer between h-BN particles and epoxy. There are slight variations in flexural strength of the nano-sized h-BN reinforced epoxy composites; however, the increasing loading level of the micron-sized h-BN particles significantly degrades the flexural strength of the epoxy. The degradation of flexural strengths could be attributed to three different reasons. The first reason is the nonuniform distribution or agglomeration of the h-BN in the epoxy matrix, which was previously confirmed by Han et al. [3] using BN-nanosheets in the epoxy matrix. The second reason can be considered a poor interfacial adhesion between h-BN particles and epoxy matrices, making it hard to transfer and distribute the applied load in the matrix uniformly, and this problem was solved previously by surface treatment of BN particles by Wattanakul et al. [28]. The last reason could be specified for only the bending test, where the activation of simultaneous compression and tension stresses in the bending test causes a decrease in bending strength.

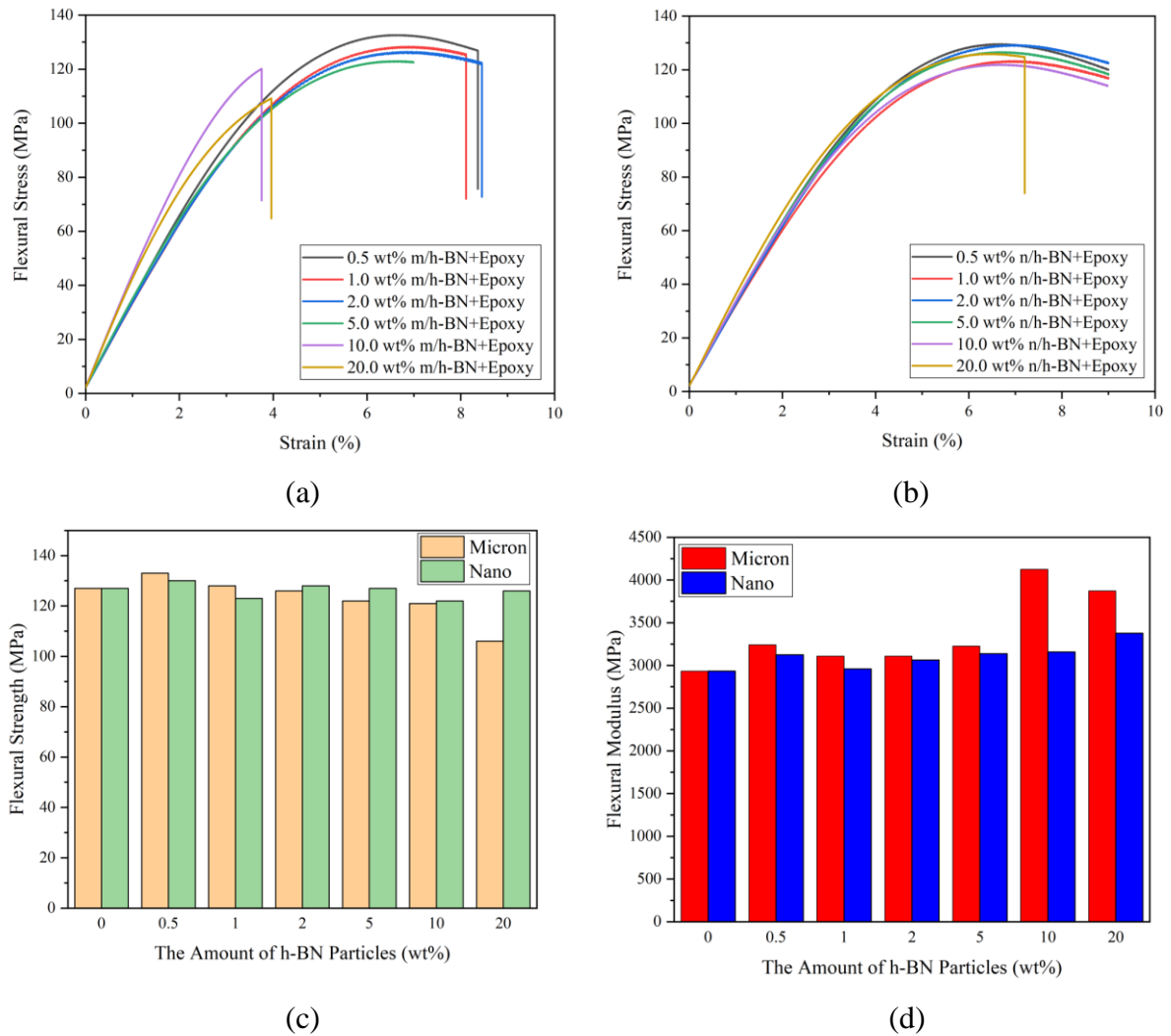


Figure 8. Flexural stress-strain curves of (a) micron- and (b) nano-sized h-BN epoxy composites as a function of different loadings, and comparison of (c) flexural strength improvement and (d) flexural modulus improvement in terms of micron- and nano-sized h-BN particles

Table 4. Flexural modulus and strength values and their improvements of micron-sized h-BN particles reinforced epoxy composites as a function of loading ratio

Sample	Flexural modulus (MPa)	Improvement (%)	Flexural strength (MPa)	Improvement (%)
Neat epoxy	2934±93.8	-	127±2.1	-
0.5 wt% m/h-BN+Epoxy	3241±9.5	10.46	133±0.7	4.72

1.0 wt% m/h-BN+Epoxy	3109±42.4	5.96	128±1.77	0.79
2.0 wt% m/h-BN+Epoxy	3119±19.7	6.31	126±1.03	-0.79
5.0 wt% m/h-BN+Epoxy	3227±11.1	9.98	122±2.49	-3.94
10.0 wt% m/h-BN+Epoxy	4126±47.7	40.63	121±3.01	-4.72
20.0 wt% m/h-BN+Epoxy	3872±83.7	31.97	106±2.30	-16.54

Table 5. Flexural modulus and strength values and their improvements of nano-sized h-BN particles reinforced epoxy composites as a function of loading ratio

Sample	Flexural modulus (MPa)	Improvement (%)	Flexural strength (MPa)	Improvement (%)
0.5 wt% n/h-BN+Epoxy	3124±39.0	6.48	130±1.15	2.36
1.0 wt% n/h-BN+Epoxy	2959±22.2	0.85	123±0.83	-3.15
2.0 wt% n/h-BN+Epoxy	3065±41.8	4.46	128±1.47	0.79
5.0 wt% n/h-BN+Epoxy	3138±12.8	6.95	127±0.78	0.0
10.0 wt% n/h-BN+Epoxy	3159±39.9	7.67	122±1.25	-3.94
20.0 wt% n/h-BN+Epoxy	3378±52.0	15.13	126±1.08	-0.79

Dynamical mechanical analysis (DMA) is an effective, versatile, and sensitive technique utilized for the determination of the thermomechanical properties, and molecular relaxation processes of polymeric materials. The oscillatory stress is applied to the samples, and storage modulus (E') and loss modulus (E'') are defined through strain measurement as a response to applied periodic stress. The ratio of the loss modulus to storage modulus gives the loss factor ($\tan\delta$ or damping ratio) and the peak point of loss factor vs temperature graphs corresponds to glass transition temperature (T_g), which specifies the maximum service temperature of the polymeric materials [29].

Fig. 9a and 9b demonstrate the variation of the storage modulus of epoxy as a function of temperature, particle size, and concentration of h-BN particles. The storage modulus, which can be assumed from the elastic modulus, is directly proportional to the amount of micron- and nano-sized h-BN particles. The enhancement in the storage modulus is

attributed to improvement in the load-bearing capacity and stiffness of the epoxy by the addition of the high stiff h-BN particles, and the increment in the concentration level of h-BN particles enables a high number of particles connected to epoxy [30]. Furthermore, the homogeneous dispersion of rigid h-BN particles establishes efficient load transfer pathways, thereby load transfer is facilitated through the h-BN/epoxy interfaces. In addition, the chemical bonds between h-BN particles and epoxy restrict the molecular chain mobility of epoxy in nearby places to h-BN particles whereby storage modulus is enhanced [31][32]. The storage modulus starts to decline with increasing temperature due to relaxation in the molecular mobility of epoxy chains, and then a sharp decrease takes place in a high-temperature range, which is designated as the glass transition region [33]. The glass transition temperature is a temperature range where polymer chains go from a glassy state to a rubbery state [3].

The variation of loss factor with temperature is presented in Fig. 9c and 9d, and the T_g values of samples can be compared as a function of particle size and concentration of h-BN particles according to peak points of the graphs. The T_g is a property associated with the molecular mobility of polymers which is affected by chain rigidity, linearity, and packing. Fig. 9c and 5d show the mild variations in T_g of the epoxy composites with the addition of the micron- and nano-sized h-BN particles. The slight improvements refer to the restriction of segmental motion of polymer chains at locations near the filler-matrix interface [34]. In contrast, the moderate decrease is explained by the reduction of the cross-linked density in the composite and low interfacial interaction between h-BN particles and epoxy matrix [35].

Furthermore, the highness of the $\tan\delta$ is a sign of the energy dissipation characteristics of the materials. Fig. 9c and 9d show that the highness of the $\tan\delta$ increases with the addition of micron- and nano-sized h-BN particles, and the maximum highness value was obtained in the epoxy with 10 wt% of micron-sized h-BN. This increment can be attributed to the interaction between h-BN and epoxy molecules, whereby low highness indicates a strong interaction [36]. As a result of the strong interaction, the chain entanglement is observed nearby places to fillers; thereby, chain mobility of the epoxy is prevented.

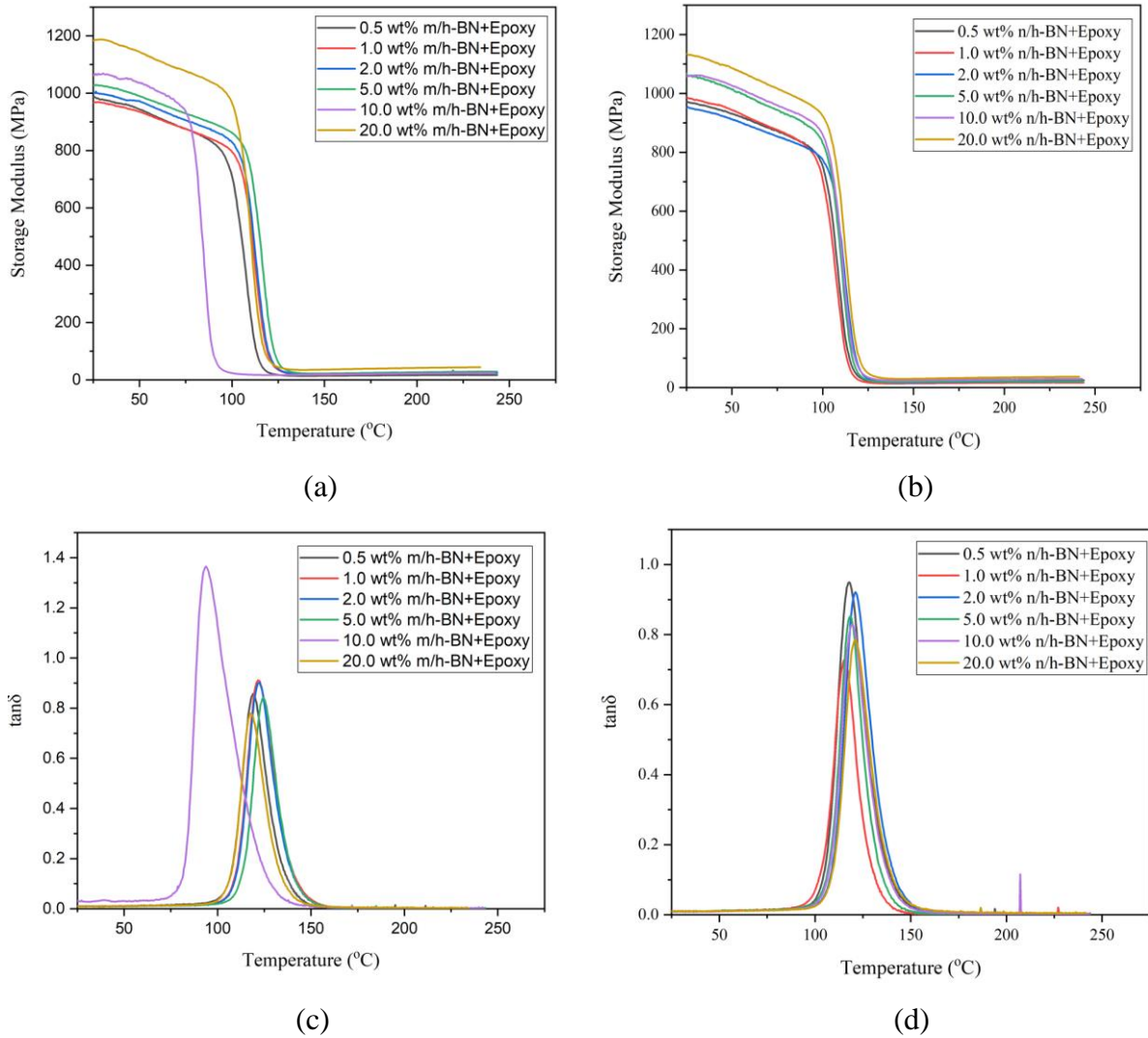


Figure 9. Temperature sweep of the storage modulus of (a) micron-sized and (b) nano-sized h-BN reinforced epoxy composites, and damping ratio curves of (c) micron-sized and (d) nano-sized h-BN reinforced epoxy composites

2.3.3. Tailored thermal conductivity of epoxy composites as a function of particle size and loading ratio of h-BN particles

Since composite materials contain different types of materials in their structures, the intrinsic thermal conductivity values of filler and matrix, concentration, particle size, and shape of filler play critical roles in the thermal conductivity values of final composites [37]. The thermal conductivity properties of composite materials are enhanced by establishing highly thermal conductive pathways, minimization of interfacial resistance between filler and matrix, and thermal resistance arising from lattice defect, impurity, boundary, and phonon-phonon scattering through conductive pathways [35][38]. Fig. 10a

and 10b show the thermal conductivity values of epoxy in in-plane and through-thickness directions as a function of particles size and concentration of h-BN particles. In both directions and at all concentration levels, the micron-sized h-BN reinforced epoxy exhibits higher thermal conductivity values than those of nano-sized. The heat transport phenomenon is associated with phonon flow in non-metals, and the higher particle size of the micron-sized h-BN limits the number of interfacial areas between h-BN and epoxy; hence, the phonon scattering is diminished through the conductive pathways, and the thermal conductivity shows significant enhancement for particles with wider interfacial surface areas [39]. Furthermore, the large particles also construct thick and highly stable conductive pathways, and other particles cannot disrupt this at the boundary of the conductive pathways [40].

As another factor, the thermal conductivity values are improved by increasing the loading levels of both micron- and nano-sized h-BN particles; however, these values follow a non-linear way whereby the improvement percentage is higher for high loading levels than those at lower loading levels, as seen in Fig. 10a and 10b. This circumstance is explained by initiation to establish thermally conductive pathways thanks to filler connections at high filler concentration levels [41]. The thermal conductivity values of the neat epoxy are 0.222 W/m.K in in-plane and 0.231 W/m.K in the through-thickness direction, and the differences between these two directions are attributed to molecular chain alignments of the epoxy. Besides, the thermal conductivity values show enhancement by utilizing micron- and nano-sized h-BN particles, and the maximum values of in-plane and through-thickness are 0.46 W/m.K and 0.49 W/m.K, respectively, with an increase of 107.2% and 112.1% for 20 wt% of micron-sized h-BN which are approximately two times higher than those of nano-sized.

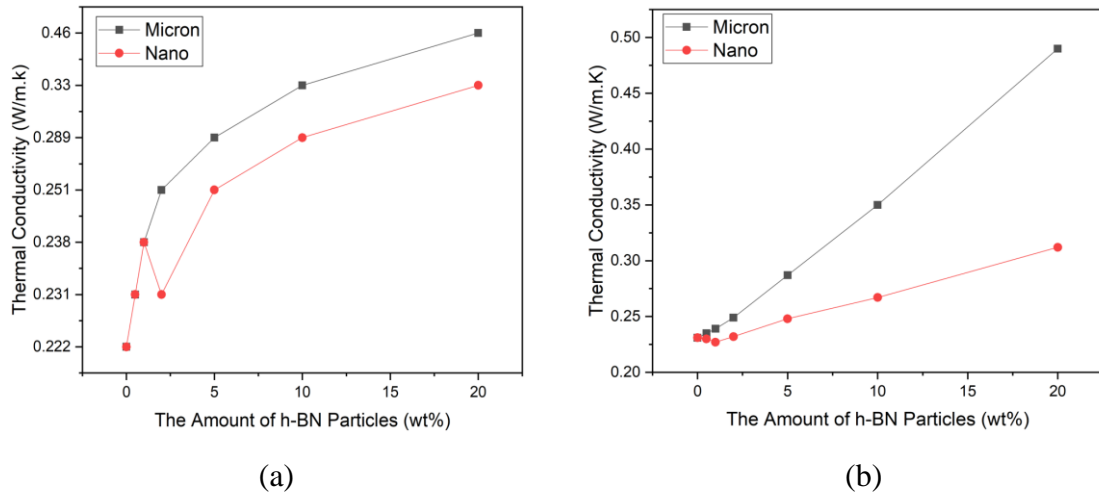


Figure 10. The comparison of the thermal conductivity values of the epoxy composites in (a) in-plane (b) through-thickness directions as a function of particle size and concentration of h-BN particles

Table 6. The thermal conductivity of micron-sized h-BN reinforced epoxy composites in in-plane and through-thickness directions as a function of loading ratio

Samples	In-Plane Thermal Conductivity (W/m.K)	Improvement (%)	Through-Thickness Thermal Conductivity (W/m.K)	Improvement (%)
Neat Epoxy	0.222	---	0.231	---
0.5 wt% m/h-BN+Epoxy	0.231	4.1	0.235	1.7
1.0 wt% m/h-BN+Epoxy	0.238	7.2	0.239	3.5
2.0 wt% m/h-BN+Epoxy	0.251	13.1	0.249	7.8
5.0 wt% m/h-BN+Epoxy	0.289	30.2	0.287	24.2
10.0 wt% m/h-BN+Epoxy	0.330	48.6	0.350	51.5
20.0 wt% m/h-BN+Epoxy	0.460	107.2	0.490	112.1

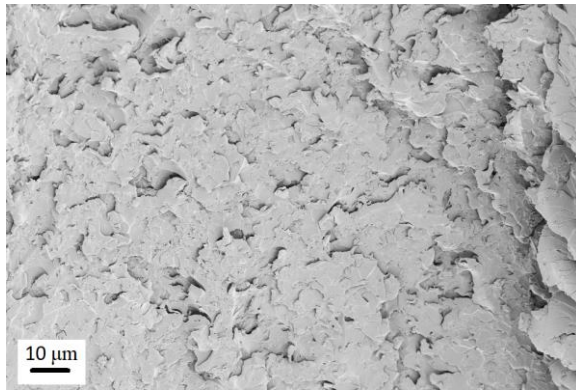
Table 7. The thermal conductivity of nano-sized h-BN reinforced epoxy composites in in-plane and through-thickness directions as a function of loading ratio

Samples	In-Plane Thermal Conductivity (W/m.K)	Improvement (%)	Through-Thickness Thermal Conductivity (W/m.K)	Improvement (%)
0.5 wt% n/h-BN+Epoxy	0.224	0.9	0.230	-0.4
1.0 wt% n/h-BN+Epoxy	0.223	0.5	0.227	-1.7
2.0 wt% n/h-BN+Epoxy	0.224	0.9	0.232	0.4
5.0 wt% n/h-BN+Epoxy	0.252	13.5	0.248	7.4
10.0 wt% n/h-BN+Epoxy	0.257	15.8	0.267	15.6
20.0 wt% n/h-BN+Epoxy	0.312	40.5	0.312	35.1

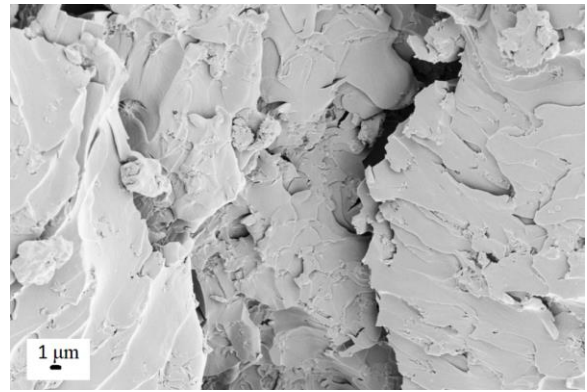
2.3.4. Fracture surface analysis of neat and h-BN reinforced epoxy composites in terms of micron- and nano-sized h-BN particles

Fracture surface analysis establishes a deep understanding of the dispersion states of micron- and nano-sized h-BN in epoxy and the failure behaviors of final composites. Fig. 11 demonstrates SEM images of the neat epoxy fracture surfaces, 10 wt% micron-sized h-BN reinforced epoxy, and 10 wt% nano-sized h-BN reinforced epoxy after the tensile test. Fig. 11a and 11b exhibit the fracture surface morphology of the neat epoxy specimen at different magnifications, and the rough surface, which is characteristic of ductile breakage, indicates the high fracture toughness. Fig. 11c and 11d show fracture surfaces of 10 wt% micron-sized h-BN reinforced epoxy composite, and the smooth surface implying the brittle breakage nature of the sample is observed. As mentioned previously, the composite material, including 10 wt% micron-sized h-BN, is more brittle than neat epoxy according to elastic modulus, which is confirmed by SEM images. On the other hand, the fracture surface of the nano-sized h-BN reinforced epoxy has significantly

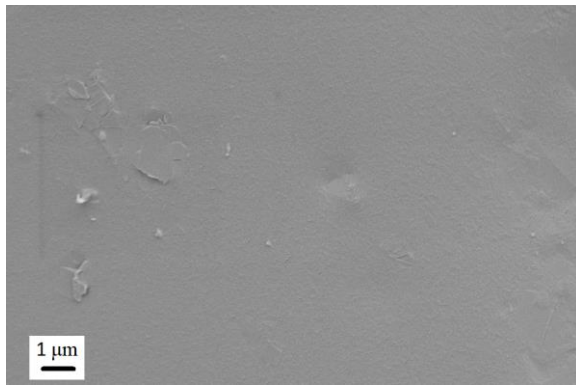
rougher than the other specimens, as shown in Fig. 11e and 11f, and the roughness is correlated with toughening and additional surface formation during the crack mechanisms. In addition, the crack deflection, twisting, and tilting lead to the formation of the rough surface area, and this surface morphology points out the efficient energy dissipation characteristic. Moreover, uniform roughness implies the homogeneous dispersion of h-BN in epoxy without any observable agglomerations and tight interfacial bonding between nano-sized h-BN and epoxy [42].



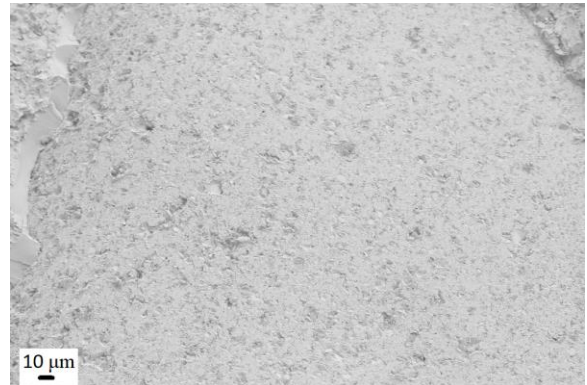
(a)



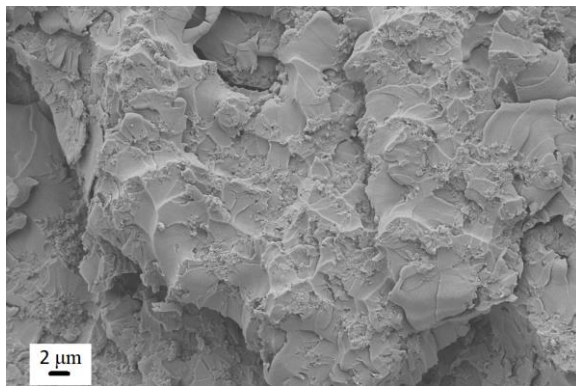
(b)



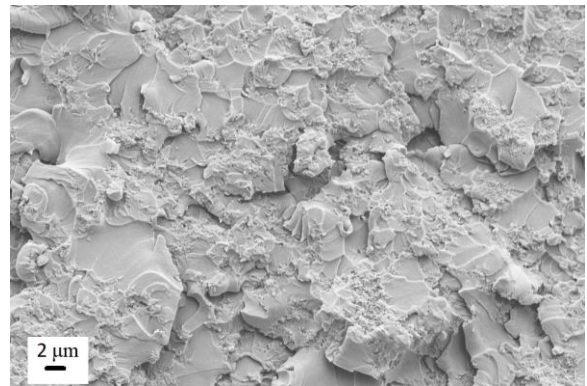
(c)



(d)



(e)



(f)

Figure 11. SEM images of the fracture surfaces after tensile test (a,b) neat epoxy (c,d) 10 wt% micron-sized h-BN reinforced epoxy composite, and (e,f) 10 wt% nano-sized h-BN reinforced epoxy composite

2.4. Conclusion

The fast, up-scalable, and cost-effective pre-dispersion method is employed to incorporate micron- and nano-sized h-BN in epoxy to obtain a highly dispersed and stable h-BN/epoxy mixture. The dispersion of h-BN particles in epoxy facilitates the heat and load transfer through the composite, whereby thermal and mechanical properties of the composites are remarkably enhanced thanks to the formation of highly stable thermal conductive and load transfer pathways. Furthermore, DMA test results confirm that the dispersion of micron- and nano-sized h-BN in a wide weight range does not affect the thermomechanical characteristics of epoxy; thereby, the thermal consistency of epoxy is preserved even in high temperatures.

The effect of particle size and concentration level of h-BN particles on epoxy were investigated to attain high thermal performance with optimum mechanical properties. The incorporation of the micron- and nano-sized h-BN is carried out by pre-dispersion method using probe sonication to avoid aggregation of particles in epoxy; subsequently, the epoxy composites were manufactured for thermal characterizations and mechanical tests by the classical molding method. Micron- and nano-sized h-BN integration in epoxy lead to significant improvement via increasing concentration in the thermal conductivity; on the other hand, the thermal performances of the epoxy reinforced with micron-sized h-BN show more noticeable performance. For instance, the thermal conductivity of epoxy is enhanced by 107% and 112% in in-plane through-thickness directions for the 20 wt% micron-sized h-BN, respectively, while the nano-sized h-BN reinforced epoxy shows 41% improvement in both directions when compared to neat epoxy. Besides the thermal conductivity analysis, tensile and 3-point bending tests are carried out to determine optimum h-BN particle size distribution and concentration for mechanical behaviors with high thermal conductivity. Epoxy modified with 20 wt% micron-sized h-BN shows 47% improvement in tensile modulus, and epoxy including 10 wt% micron-sized h-BN has 41% enhancement in flexural modulus. In contrast, 20 wt% nano-sized h-BN concentration improves the tensile and flexural modulus values of epoxy by 16% and 15%, respectively. The fractography analyses were detailly carried out to investigate the effect of particle size, interfacial interaction between filler and matrix, dispersion quality, as well as the concentration level of h-BN particles on the fracture mechanism of composites under tensile load. This novel research provides a deep understanding of the synergistic effect of particle size and concentration of h-BN particles on the most common

thermoset polymeric materials like epoxy. It is considered that these results will be a guideway, especially in to be produced multi-scale composites consisting of fibers and h-BN particles, as well as the surface treatment works. Furthermore, it is strongly believed that this state-of-the-art study fills in the gap in the literature on the particle size-concentration relationship investigation of inorganic thermally conductive fillers such as h-BN particle used as primary reinforcement agent for thermoset composites with notable mechanical properties.

CHAPTER 3. THE SYNERGISTIC EFFECT OF CARBON NANOMATERIAL COATED GLASS FIBERS ON THE PERFORMANCE OF EPOXY COMPOSITES HAVING h-BN PARTICLES

Four different arrangements are determined to fabricate multi-scale epoxy composites in which micron-sized h-BN particles and nano-sized SWCNT are utilized in resin and interfaces of glass fibers as primary modifiers, respectively. In the first design, the pre-dispersion method is used to incorporate the micron-sized h-BN particles in epoxy resin. Homogeneous and highly stable dispersion of h-BN particles in epoxy improves the thermal and mechanical properties through efficient heat and load transfer between glass fibers and epoxy. In the second design, the SWCNT is coated onto glass fibers by dip coating to prevent a thermal mismatch between glass fibers and epoxy. In the third design, the neat and SWCNT coated glass fibers are utilized together as a hybrid system to evaluate the gradual increment in the thermal and mechanical properties of the composites. In the last design, the combination of the hybrid system and h-BN reinforced epoxy is studied to obtain promising thermal conductivity as a multi-scale composite. The synergistic effects of the h-BN particles and SWCNT as resin and interface coating modifiers are examined by carrying out several physical and chemical characterization methods. The usage of h-BN particles for all designs improves the thermal performance in in-plane and through-thickness directions. The hybrid systems with h-BN particles show remarkable enhancement in thermal conductivity in through-thickness direction by 32%.

3.1. Experimental

3.1.1. Materials

Micron-sized h-BN particles in the average particle size of 4-10 μm and commercial SWCNT suspensions with a concentration of 0.2 wt% were purchased from Civelek Porselen Company from Turkey, and OcSiAl Company-Pinhas Company, from Turkey, respectively. Ethanol (99%) to utilize for dispersion of micron-sized h-BN was purchased from Sigma Aldrich. Sika Biresin® CR131 and CH132-5 hardener two-part system were supplied by Tekno Chemicals Inc. This resin system was selected for the vacuum infusion process owing to its high T_g and low viscosity. Bidirectional E glass plain woven were supplied by Metyx.

3.1.2. The selective dispersion of micron-sized h-BN and SWCNT in resin and fiber interfaces

Two different incorporation procedures were performed to fabricate the multi-scale composites containing h-BN and SWCNT particles. In the incorporation of h-BN particles, 10 wt% loading level was selected since epoxy composites, including micron-sized h-BN particles in this concentration, have promising thermal conductivity values in in-plane and in through-thickness directions supported by high mechanical properties as explained in the previous section. Firstly, micron-sized h-BN was dispersed in ethanol, and a homogeneous mixture was prepared using an ultrasonicator (Hielscher UP400S) for 1 h at room temperature. Subsequently, this solution was mixed with epoxy and sonicated for an additional 2 h. The pre-dispersion method is utilized to attain a stable and highly dispersed epoxy mixture.

In the second approach, the dip-coating method is employed to graft homogeneously SWCNT onto glass fibers to fabricate a multi-scale composite system. The supplied commercial SWCNT solution with a concentration of 0.2 wt% was firstly diluted with distilled water in the ratio of 1:1, then dilute solution was sonicated to improve the dispersion quality of the solution for 15 min at room temperature. After the coating process, the SWCNT coated glass fibers were kept in the oven at 120 °C for the drying process.

3.1.3. Preparation of Composites having different designs by Vacuum Infusion and Hand Lay-up combined with Hot Press Methods

Vacuum-assisted resin transfer method (VARTM) and hand lay-up combined with a hot press were employed for composite manufacturing as two different methods. In the first production technique, the glass fibers are stacked onto a stainless-steel infusion table, then impregnated with degassed epoxy resin while glass fibers are under a vacuum environment. Multi-scale composites in 5 different designs were produced by VARTM, and the reference neat fabric/neat resin was manufactured in the first design. In the second design, neat fabric/10 wt% m/h-BN epoxy resin was produced to observe the effect of the micron-sized h-BN on mechanical, thermal, and thermomechanical properties of composites as a matrix modifier. In addition, the other composite designs such as hybrid fabric/neat resin, hybrid fabric/10 wt% m/h-BN epoxy resin, and full coated glass fiber/neat resin are produced utilizing a combination of the neat and SWCNT coated glass fabrics with a concentration of 0.1 wt% SWCNT. In the production of reference

composite, 17 layers of glass fibers and neat epoxy resin are used for manufacturing; on the other hand, 17 layers of substitutional symmetrical design as 1 layer neat and 1 layer coated fabric are utilized in the hybrid system. The combined usage of the neat and SWCNT glass fibers is to evaluate the effect of the gradual increment of the SWCNT on thermal and mechanical properties in the system.

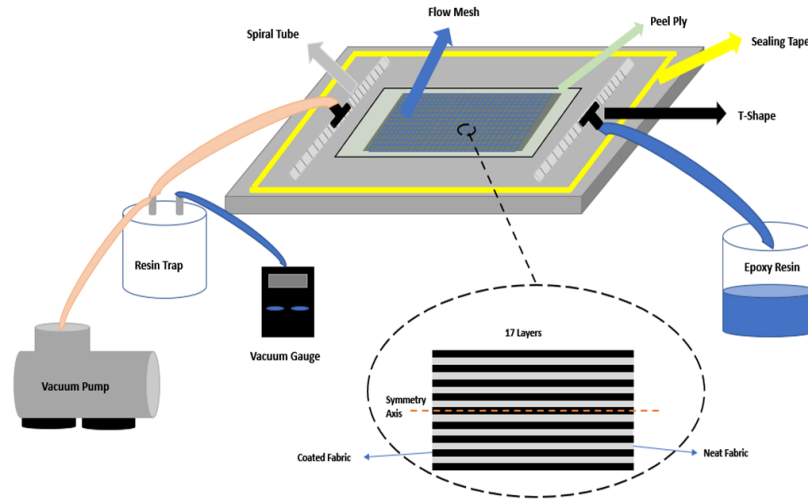


Figure 12. The schematic representation of the glass fiber reinforced composites production procedure by the vacuum infusion method

In the second production method, the hand lay-up combined with the hot press technique is conducted to fabricate composites using the same glass fiber and resin combinations. The degassed resin was applied to fibers ply by ply, and then the impregnated fibers were taken in a vacuum environment and consolidated by the hot press for 5 h at 100 °C and 2.5 tones. This method is selected to prevent filtration of h-BN particles and produce homogeneous and thick composite materials which allow optimum heat dissipation during the thermal conductivity tests.

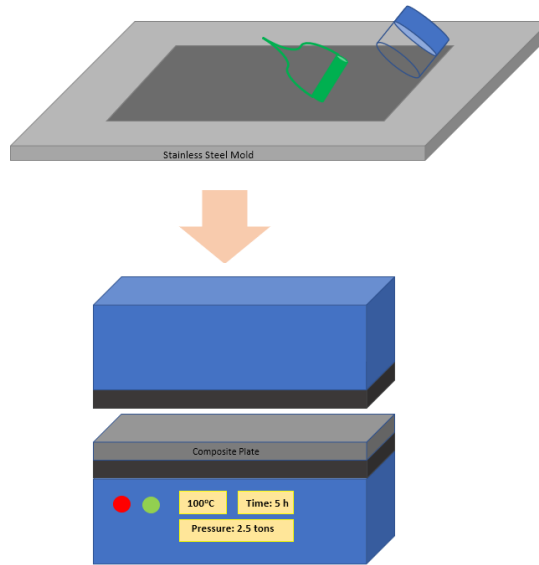


Figure 13. The schematic representation of the glass fiber reinforced composites production procedure by the hand lay-up combined with the hot press method

The produced composites are cut in 35x10x1.5 mm, 25x25x1.5 mm, and 25x25x4 mm for DMA, optical microscopy, and thermal conductivity tests, respectively, as well as tensile, flexural, and Charpy impact test specimens, are cut in 185x25x1.5 mm with a gauge length 135 mm, 70x12.7x1.5 mm, and 80x10x1.5 mm, respectively. After the cutting of tensile test specimens, the grip locations of the specimens are polished with 800-grit sandpaper to enhance the adhesion capability of samples to tab materials. Composite tab materials are selected in the dimension of 25x25x1.75 mm and adhered onto polished areas of test samples with two-component room temperature curing epoxy systems (3M Scotch-Weld Epoxy DP 490) to prevent the damage in these areas.

3.1.4. Characterization

Several microscopic and spectroscopic characterization techniques were performed to identify the properties of reinforcement materials and composite materials. The optical microscopy analysis is carried out to analyze the cross-sectional structures such as fibers orientation, voids, and resin distribution of the composite, as well as the orientation and coating quality of the glass fibers by using Nikon Eclipse LV100ND optical microscopy. After tensile test and SWCNT distribution onto glass fibers, the fracture surfaces of samples were investigated by Leo Supra 35VP Field Emission Scanning Electron Microscope (SEM, Carl Zeiss AG, Jena, Germany). FTIR spectra were conducted to determine functional groups onto neat and SWCNT coated glass fibers by using a Thermo

Scientific Nicolet iS50 FTIR spectrometer. Raman spectroscopy was performed to analyze the molecular structure, and vibrational properties of both neat and SWCNT coated glass fibers by utilizing a Renishaw inVia Reflex Raman Microscope with 532 nm edge laser at room temperature in the range of 100–3500 cm^{-1} . The density of composite parts is measured in accordance with Archimedes Principle. Thermogravimetric analysis (TGA) was carried out to examine the thermal stability and weight loss percentage of glass fibers and composites by utilizing Mettler Toledo Thermal Analyzer (TGA/DSC 3+) with a 10 $^{\circ}\text{C}/\text{min}$ heating rate from room temperature to 1000 $^{\circ}\text{C}$. Dynamic mechanical analyzer (DMA) tests were performed on the samples with a dimension of 35 mm in length and 10 mm in width using a DMA Q800 (TA Instruments, New Castle, DE) in a dual cantilever mode for viscoelastic investigation with the heating rate of 3 $^{\circ}\text{C}/\text{min}$ by initiation from room temperature to 250 $^{\circ}\text{C}$ and 1 Hz.

Moreover, in-plane and through-thickness thermal conductivity measurements of the composites having different designs are operated by the hot disc method with the TPS 2500 S device. Besides the materials characterization tests, the mechanical tests were conducted by Instron 5982 Static Universal Test Machine (UTM) with 10 kN load cells. ASTM D 5083-02, ASTM D 790, and ISO 179 test standards were utilized for tensile, 3-point bending tests, and Charpy Impact Tests, respectively. Whereas the constant cross-head speeds were 5 mm/min for tensile tests and bending tests operated with a 2 mm/min bending rate, the axial and transverse extension data were recorded using a knife-edge extensometer (Epsilon, Tech. Corp.) during the tests. Ceast 9050 impactor with a 5 Joule hammer potential energy is utilized to determine the impact strength of the manufactured composites.

3.2. Results & Discussion

3.2.1. The characteristic properties of neat and SWCNT coated glass fabrics

The optical microscopy is carried out to investigate the interfacial and morphological properties of neat and SWCNT coated glass fibers in different magnification levels because these properties of the fibers directly affect interfacial interaction with epoxy, the mechanical properties of the final composites. Fig. 15 shows the morphological situation of the neat and SWCNT coated glass fibers in low magnification. The space between adjacent fibers is very crucial because the space filled with SWCNT reduces the interfacial interaction with epoxy and leads to wettability and delamination problems.

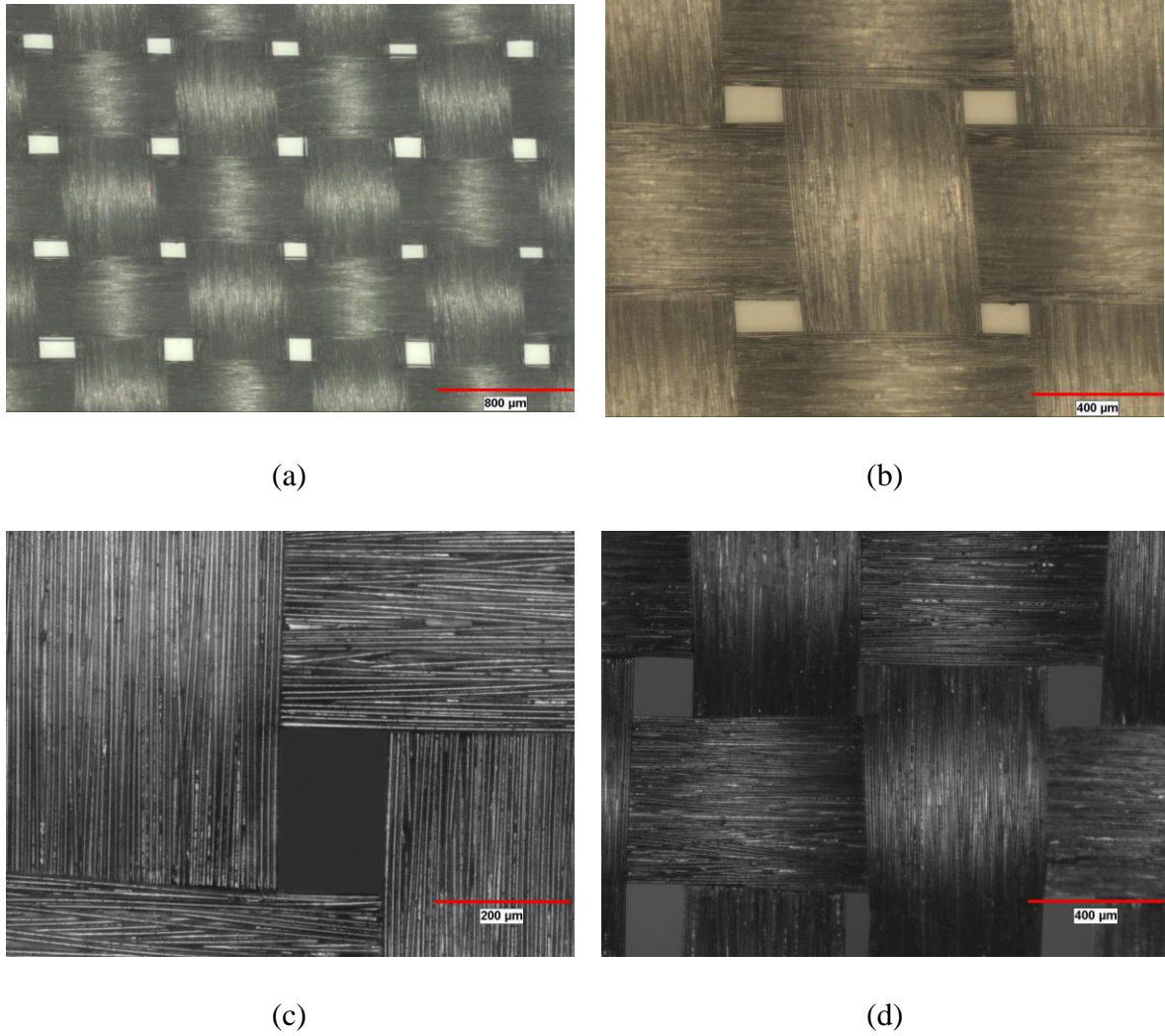


Figure 14. Optical microscopy images of glass fibers (a,b) as-received (c,d) after the SWCNT coating

SEM analysis was conducted to observe the distribution of SWCNT on fibers, interspace areas among fibers, and the effectiveness of the coating process. Fig. 16 shows SEM images of the neat and SWCNT coated glass fibers. The parallel and smooth surface alignments of the glass fibers at different magnifications are shown in Fig. 16a and 16b, and Fig. 16c and 16d exhibit the homogeneous and thin SWCNT dispersion after the dip-coating method. The coating of the SWCNT does not negatively affect the morphological properties of the glass fibers, and the glass fabrics retain their consistent structure after dip coating processes, and the chemical and physical interaction between SWCNT and glass fibers gives rise to strong attachments of the nanofillers on fibers. In addition, the van der Waals interaction among SWCNT bundles causes aggregate SWCNTs; however, the effective dispersion inhibits the formation of the agglomerations. The SWCNT increases the surface energy and roughness of the glass fibers, which provides a high

interfacial interaction between fibers and epoxy. The dip-coating method, which is utilized for the deposition of SWCNT onto glass fiber surfaces, is a solvent-based method and gives an environmentally friendly solution for producing SWCNT coated fiber by using distilled water as a dispersion medium. The dispersion quality of the solution is the critical parameter for the dip-coating method; thus, the sonication must be performed smoothly. Moreover, the drying process is also significant in terms of the structural consistency of the fibers. The evaporation of the moisture absorbed during the dip-coating process in the structure of the glass fibers takes place when the fibers are put in the oven, and tension that occurs in the drying of the fibers can damage the sensitive structure of the glass fibers. The smooth and parallel structure confirms that the process has no negative influence on the glass fibers, as seen in Fig. 16c and 16d.

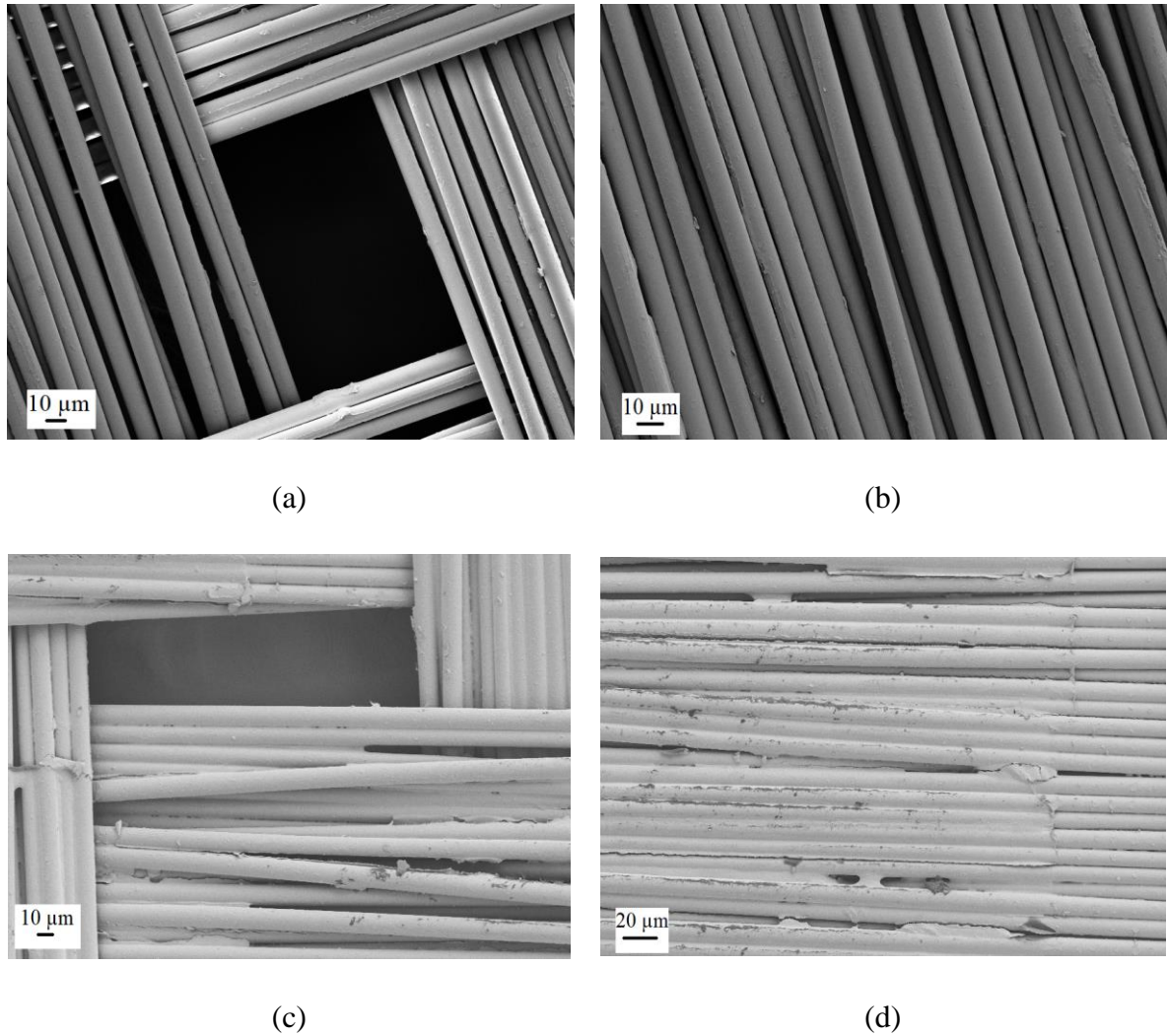


Figure 15. SEM images of the glass fibers (a,b) as-received and (c,d) after the dip-coating of SWCNT

The Raman spectra analysis was conducted to evaluate structural variations on glass fibers after coating of the SWCNT by monitoring specific CNT peaks. Fig. 18 shows the Raman spectra of SWCNT, neat, and SWCNT coated glass fibers. The glass fibers do not exhibit any specific peak in the Raman analysis; however, SWCNT has three characteristic peak points, which are radial breathing mode (RBM) at $\sim 100\text{-}200\text{ cm}^{-1}$, G which is due to in-plane stretching vibrations of C-C bond in peak at 1588 cm^{-1} and 2D peak at 2699 cm^{-1} attributed to again sp^2 bonded carbon atoms. RBM, which corresponds to out-of-plane bond stretching, cannot be seen in other graphene types because it is related to the cylindrical shape of the carbon nanotubes; in addition, the characteristic peaks of SWCNT behave as dominant by dip-coating of the glass fibers [43].

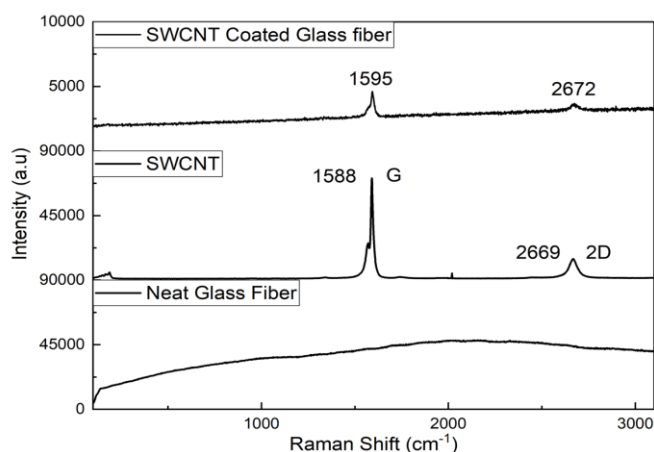


Figure 16. Raman spectra of SWCNT, neat and SWCNT coated glass fibers

TGA was performed to evaluate the thermal stability of materials, and micron-sized h-BN, neat, and SWCNT coated glass fibers were heated from room temperature to 1000 °C. Fig. 19 demonstrates the weight loss as a function of temperature. Micron-sized h-BN loss approximately 0.5% small amounts of weight until the temperature reaches 100 °C, and this behavior can be attributed to the evaporation of whole moisture in the volume of the h-BN. In addition, the TGA graph of neat glass fabric contains 2 steps. Approximately moisture, which is corresponded to 0.15% of all volume, is removed like h-BN until 100 °C in the first step, and there is a weight loss in a percentage of 0.68% in the temperature range between 200 °C-400 °C in the second step of neat glass fiber. This weight reduction refers to removing the polymer sizing agent or coupling agent in the structure of the as-received glass fibers. Furthermore, the SWCNT coated glass fabric shows weight reduction in the three steps. The first two steps have the same behavior with neat glass fabric; however, the difference is that the removed weight is in a percentage of 0.23% and a little bit higher than the neat one. In the second step, the SWCNT-coated glass fiber loses 0.7% of its weight, and 0.99% of the total amount is lost in the temperature range 400 °C-550 °C as a third step.

The amount of the nanomaterials onto glass fiber can also be calculated by TGA. The difference in the TGA curves of the neat and SWCNT coated glass fibers is in the third step of the line belonging to coated fiber. This weight reduction can be attributed to the burning of the SWCNT in the structure, and the loss percentage is 0.99%, as mentioned above. The initial weight of the utilized SWCNT coated glass fabric is 26.33 mg, and according to the initial weight of the fiber, the SWCNT amount is calculated as 0.26 mg. Besides, the 4x4 mm glass fibers are used for TGA analysis, and 20x20 mm composites

are produced during the VARTM process; consequently, it can be said that one ply of the composites contains 6.51 mg SWCNT.

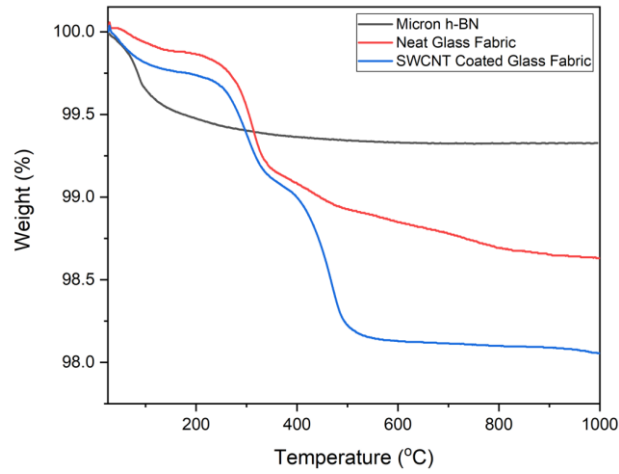
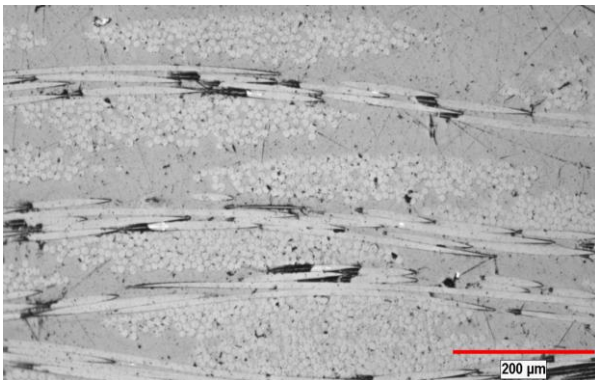


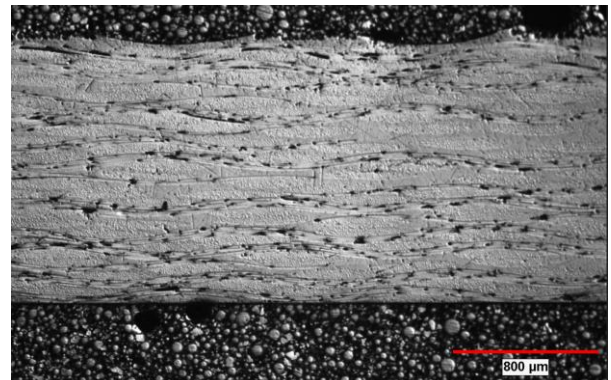
Figure 17. The percentages of weight loss of micron-sized h-BN, neat glass fabric and SWCNT coated glass fabric

3.2.2. The characteristic properties of composites having different designs

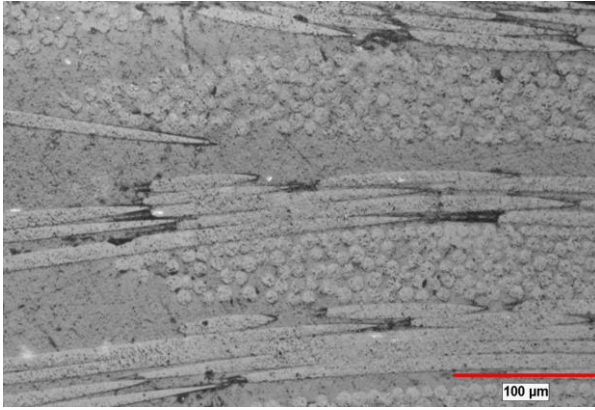
Optical microscopy analysis is conducted to observe the orientation of fibers, surface defects, and voids in the structure of the composites. Fig. 20 exhibits the optical microscopy images of the composites having different designs, and the voids and surface damages can be seen easily. In addition, the parallel alignments of the fibers are observed, and the average fiber diameter is calculated in the range of approximately 8.5-11 μm .



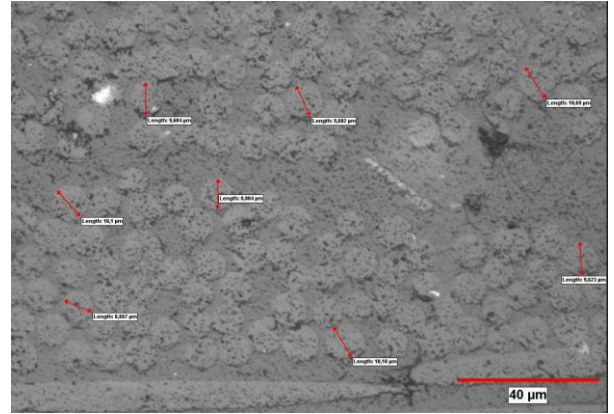
(a)



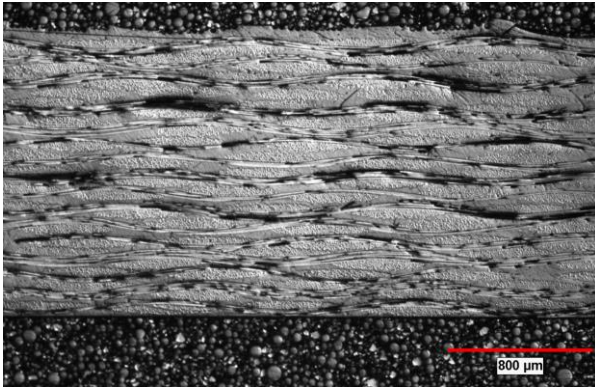
(b)



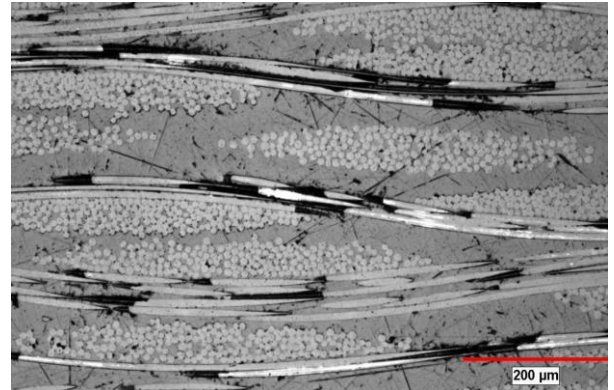
(c)



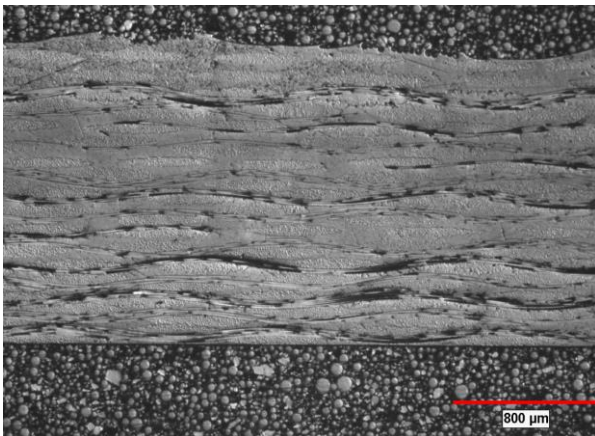
(d)



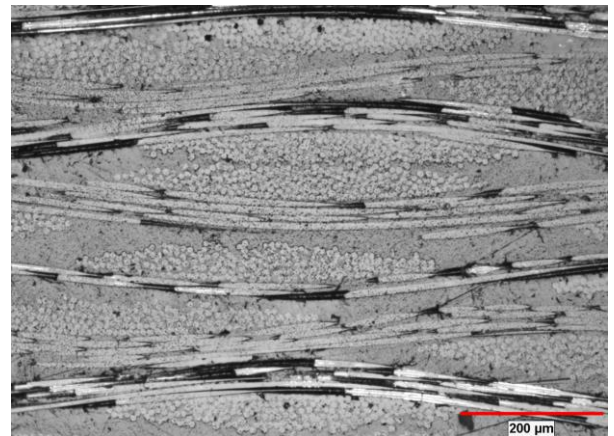
(e)



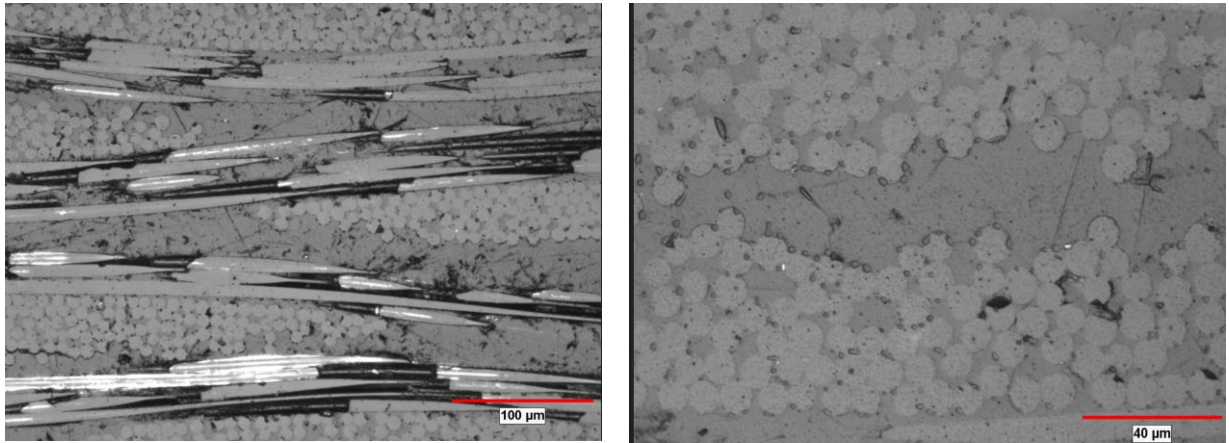
(f)



(g)



(h)



(i)

(j)

Figure 18. The optical microscopy images of the (a,b) neat fabric/neat resin (c,d) neat fabric/10 wt% m/h-BN epoxy resin (e,f) hybrid fabric/neat resin (g,h) hybrid fabric/10 wt% m/h-BN epoxy resin (i,j) full SWCNT coated fabric/neat resin

Archimedes' Principle test calculates the experimental density values of the composites with different designs. According to the Archimedes Principle test result, the highest density value is obtained for neat fabric/neat resin. There is no significant influence of h-BN on density; in contrast, the density is lowered with the increasing number of coated fabrics in the system. The lowest density value is 1.76 g/cm^3 and observed for full SWCNT coated fabric/neat resin, while the highest density value is 1.82 g/cm^3 attained for the neat fabric/neat resin system. It can be understood that as the amount of the nanomaterials increased in the composites, the density of the composites decreased. This situation can be attributed to composites with SWCNT coated glass fibers losing their rigidity which leads to a decrease in the density of the composites.

Table 8. The density values of the composite materials having different designs

Sample	Neat Fabric/Neat Epoxy Resin	Neat Fabric/10.0 wt% m/h-BN Epoxy Resin	Hybrid Fabric/Neat Epoxy Resin	Hybrid Fabric/10.0 wt% m/h-BN Epoxy Resin	Full SWCNT Coated Fabric/Neat Epoxy Resin
Density (g/cm^3)	1.82	1.81	1.79	1.79	1.76

TGA was employed to investigate the thermal stability of the composites with different designs starting from room temperature to 800 °C. Fig. 21 shows the weight loss percentage variations of the composites having different designs with increasing temperature, and all composites have one stepped decomposition curve. The composites start to decompose at 150 °C, and degradation finalizes at approximately 400 °C. Furthermore, the remaining weight of the composites including h-BN particles is the highest; on the other hand, the SWCNT coated glass fiber reinforced composite exhibits the higher weight reduction. This behavior is attributed to h-BN particles are not affected by temperature like glass fibers; however, the SWCNT coating is burnt with epoxy at decomposition temperature range. In addition, the weight reduction differences between composites are low, which explains that the high amount of h-BN particles in the resin are infiltrated during the vacuum infusion processes.

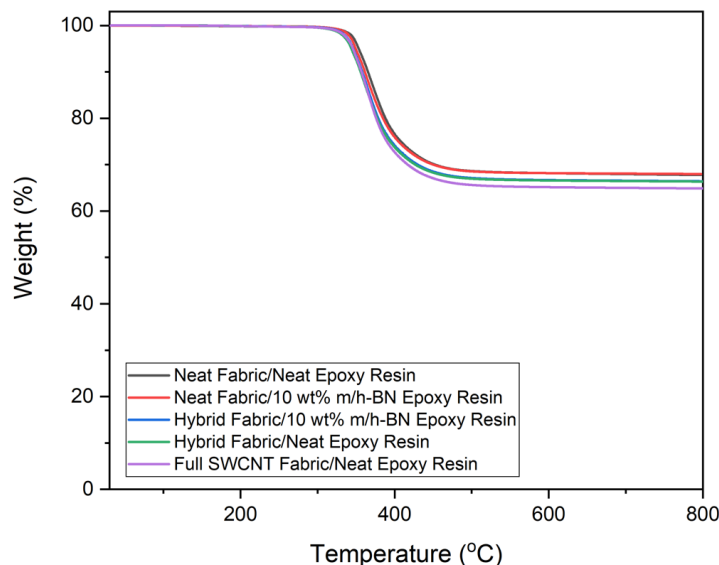


Figure 19. The weight loss percentage variations of the composites having different designs with temperature

3.2.3. The effect of the h-BN and SWCNT on the mechanical and thermomechanical properties of composites having different designs in resin and interface

A high number of interfacial areas are situated in the composite materials since composites include fiber, matrix, and filler materials in their structures. The final mechanical and thermomechanical properties of the composites are influenced by the inherent properties of the constituents and interfacial properties; hence, the covalent and noncovalent interfacial interactions between fibers and matrix have a crucial role in

composites. The adhesive interaction energy must be higher than the cohesive interaction energy of the matrix to attain rigid composite structures, and secondary bondings such as Van der Waals and hydrogen increase the strength of adhesive interaction [44]. Furthermore, the interfacial interaction and homogeneous dispersion of the nanomaterials in resin and interface are very significant parameters to affect the mechanical performances of the composites [45].

The tensile strength, modulus, and strain values are given in Table 9. The strength values are improved by the addition of h-BN into epoxy resin and deposition of the SWCNT onto glass fibers. The highest enhancement with a percentage of 13.01% is obtained for neat fabric/10 wt% m/h-BN epoxy resin composite, whereas the hybrid fabric/10 wt% m/h-BN epoxy resin shows 9.00% improvement. The enhancement of the tensile strength can be attributed to the high interaction between h-BN particles and epoxy matrix, and the homogeneous dispersion of the h-BN limits the stress concentration area formation and improves the interfacial adhesion among filler and matrix [46][47]. Furthermore, h-BN particles, which are an obstacle to inhibit the crack propagation, absorb fracture energy in the matrix and behave as a stress transfer media between matrix and fibers; thereby, the mechanical performance of the composites shows enhancement [2][48]. The particles in the matrix have binding joint properties and increase the needed energy for the propagation of cracks through the matrix, and the mechanical properties exhibits improvement; however, the tensile behaviors of the composites are fiber-dominated properties, and the variation in the matrix properties can moderately affect the tensile behavior of the final composites [48].

The fiber/matrix interfacial areas behave as crack initiation sites due to the important brittleness differences among fibers and matrix [48]. The surface of the glass fibers is coated with SWCNT to inhibit the mechanical properties mismatch in the composites; nevertheless, Table 9 shows that tensile modulus values decrease with increasing amounts of the nanomaterials in the composites. The weak physical and chemical interactions inhibit the efficient load transfer at fiber-matrix interfaces, and delamination is observed in interfacial areas of the composites, including SWCNT coated glass fibers [49]. In addition, the deterioration in the tensile modulus is observed by the addition of h-BN particles in the matrix of the composites, and this deterioration in the modulus can be explained by the agglomeration of the nanofillers and void formation in the matrix. The agglomeration and void in the composite structure disrupt the matrix continuity and

diminish the wettability of the matrix to fibers, and this causes low interfacial interaction [50][51]. Moreover, the addition of a high percentage of h-BN particles increases the viscosity, which reduces the wettability of the resin, and removing the entrapped air becomes more difficult than neat epoxy resin, whereby high viscosity restricts the efficient load transfer [52]. The vacuum-assisted production techniques also improve the adhesion between fibers and epoxy since the void in the resin is removed by vacuum and provides smooth interfacial interaction areas [53].

Fig. 22a shows the tensile stress-strain curves of composites with different designs, and the neat fabric/neat resin and neat fabric/10 wt% m/h-BN epoxy resin have cracking in one step, while the composites containing SWCNT coated exhibit stepped failure. The variations in the failure behavior are signs that composites, including neat fabric, show failures with fiber breakage; on the other hand, the composites with SWCNT coated glass fiber are exposed to delamination with external stress. The strain value shows increment with the incorporation of the micron- and nano-sized reinforcement, which increase the toughness of the composites.

Table 9. Tensile strength, modulus, and strain values and their improvement percentages of the glass fiber reinforced composites as a function of usage of the h-BN and SWCNT in resin and interfaces

Sample	Tensile Strength (MPa)	Improvement (%)	Elastic Modulus (GPa)	Improvement (%)	Tensile Strain (%)	Improvement (%)	Poisson Ratio (mm/mm)
Neat Fabric/Neat Epoxy Resin	442.75±57	-	22.61±0.6	-	3.04	-	0.14
Neat Fabric/10.0 wt% m/h-BN Epoxy Resin	500.36±16	13.01	21.56±0.2	-4.64	3.72	22.37	0.13
Hybrid Fabric/Neat Epoxy Resin	469.94 ±29	6.14	20.42±0.1	-9.68	3.65	20.07	0.11
Hybrid Fabric/10.0	482.59±22	9.00	20.26±0.2	-10.39	3.99	31.25	0.12

wt% m/h-BN Epoxy Resin							
Full SWCNT Coated Fabric/Neat Epoxy Resin	455.65±5	2.91	18.38±0.1	-18.71	4.20	38.15	0.11

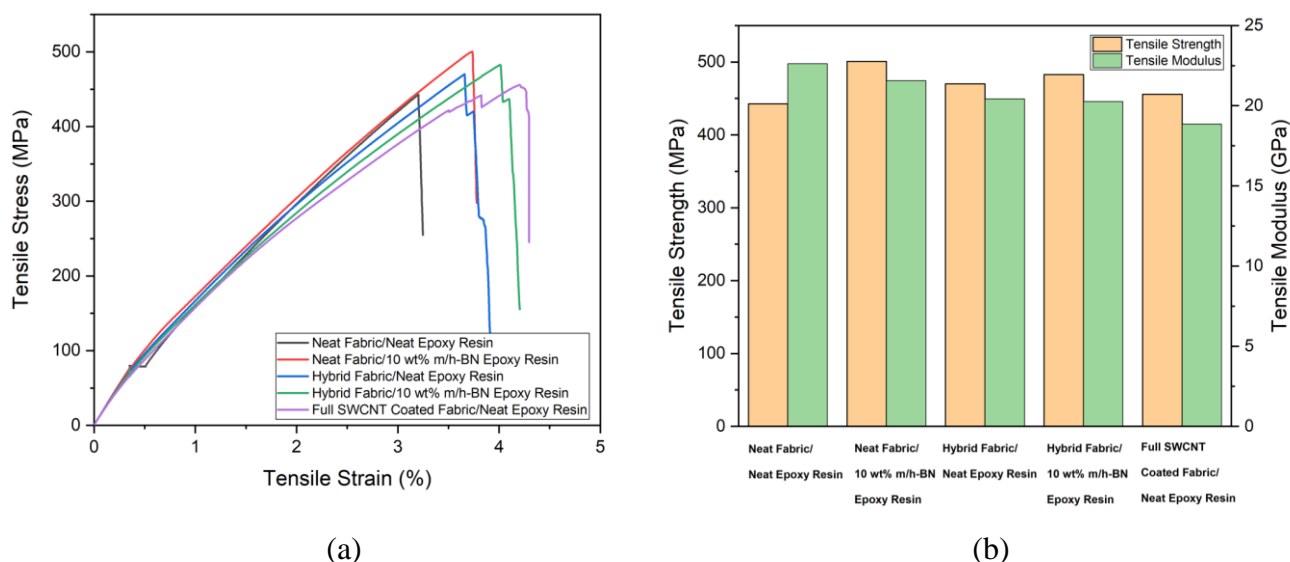


Figure 20. (a) Tensile stress-strain curves, and (b) tensile strength and modulus improvements of the composites having different designs

The 3-point bending test is utilized to evaluate the effects of the h-BN incorporation in resin and SWCNT coating on fiber surface on composite properties under flexural load. The flexural properties of the composites are matrix dominated properties, and the flexural strength, and modulus, improvements of the composites with different designs are given in Figure 23.

As a first parameter, the effect of the h-BN dispersion on flexural properties is investigated. Whereas the flexural strength shows a slight 1.79% increment, the strain values show a significant improvement of 19.71% with the addition of the h-BN in the neat fabric/neat resin. Also, hybrid fabric/10 wt% m/h-BN epoxy resin exhibits higher flexural properties with respect to hybrid fabric/neat resin. The dispersion quality directly affects the flexural strength and modulus of the composites, and the high dispersion quality increases the flexural properties [54]. Furthermore, the flexural strength can be reduced due to the agglomeration of the particles, and the agglomerations cause stress concentration areas as well as the voids in the structure. Also, the high amount of filler

materials increases the viscosity of the resin, and this situation negatively affects the wetting process of the fibers, and creates voids in the structure [55]. The higher viscosity that resin has, the degasification of the resin and impregnation of the fibers by resin is more difficult [56]. The deterioration of the interfacial adhesion capability due to the wetting properties of the resin directly influences the stress transfer efficiency of the composite [57]. In addition, the fiber pullouts and breakage are limited by the strong interfacial interaction between the fibers and epoxy, thus flexural properties show increment thanks to effective stress transfer [50].

In the second parameter, SWCNT coating on the fiber surface by the dip-coating method deteriorates the flexural properties. The strong interaction between carbon nanotubes and matrix as well as fibers is the key to obtaining maximum strength. The incorporation of the nanomaterials on the surface of the fibers establishes a bridge between matrix and fiber materials to reduce the properties mismatch and allow the efficient load transfer between constituents [58]. Normally, the continuous SWCNT coating of the glass fibers without agglomeration is expected to improve the adhesion between epoxy and glass fibers through the covalent bonding between SWCNT and fibers [59]. However, Fig. 23b shows that the flexural properties are degraded by the coating of SWCNT on glass fibers. The degradation in the flexural properties can be attributed to decreasing interfacial interaction between fibers and matrix after the coating processes, which leads to poor interaction and delamination during the flexural test.

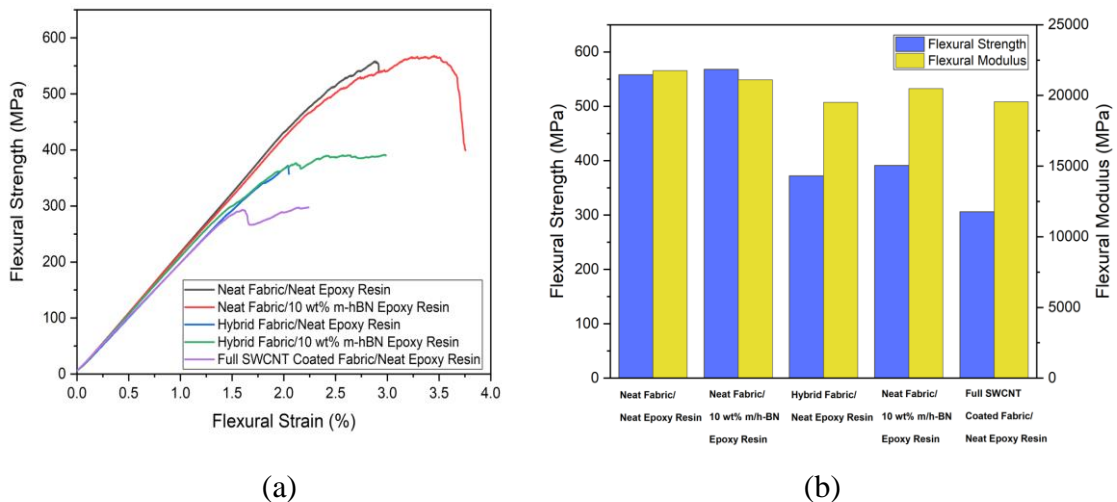


Figure 21. (a) Flexural stress-strain curves (b) flexural strength and modulus improvements of the composites having different designs

The Charpy impact test is carried out to evaluate the impact strength and energy absorption capabilities of the composites with different designs using a pendulum hammer, thanks to its cost-effectiveness and simplicity. The impact strength and energy absorption characteristics give information about the toughness or brittleness of the composites [60].

The effects of sizing of glass fibers and matrix reinforcements on composite are determined by the impact test, as seen in Fig. 24 Charpy impact strength is 17.68% enhanced via incorporation of h-BN particles in neat glass/neat resin and is 140.37 kJ/m² for the full SWCNT coated fabric/neat resin with an approximately 86% improvement. When the number of the SWCNT coated fibers increases in the structure, the impact strength shows enhancement, which can be attributed to the stress distribution of the composites developed; thus, the toughness properties of the composites are enhanced by the usage of the coated fabric. The composites with many interfacial defects are cracked even if small loads are applied to samples due to weak interfacial interaction between fibers and resin. The carbon nanotube deposited at the interfaces deviates the crack propagation direction and inhibits the contact of the crack tip with fibers. Moreover, interfacial adhesion and rigidity, as well as the stress field of the crack tip, influence the crack propagation direction; on the other hand, the improvement in the adhesion capability between fibers and resin cannot always enhance the impact strength [61][62]. As another, the usage of the h-BN improves the impact strength of composites through enhancement of the interfacial adhesion of the fibers with epoxy, inhibition of crack propagation, and bridging effect on the defects; nevertheless, the high amount of h-BN particles form the agglomeration, which causes stress concentration areas and inhibition of the effective stress transfer [63][64].

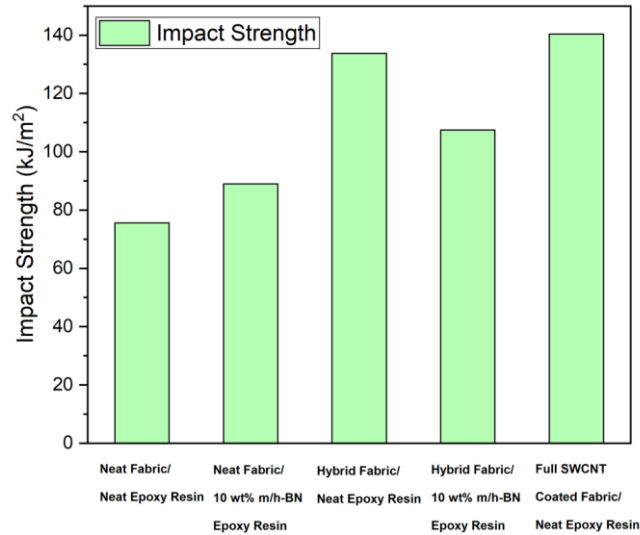


Figure 22. The impact strength variations of the composites in terms of the h-BN and SWCNT utilization in resin and interfaces

Dynamical mechanical analysis (DMA) is an effective technique utilized to determine the thermomechanical properties of polymeric materials. The oscillatory stress is applied to polymeric materials to calculate the storage modulus (E') and loss modulus (E'') of the materials by means of strain measurement. The ratio of the loss modulus to storage modulus gives the damping ratio, and the peak point of this phenomenon corresponds to the glass transition temperature (T_g) of the materials [65]. The composite materials are composed of different materials, and properties like fiber-matrix interface, fiber orientation, and filler loading influence the thermomechanical properties of fiber-reinforced composites. In addition, relaxation and transition processes, as well as the microstructure of the composites, have effects on the viscoelastic properties of the composites [66].

Fig. 25a shows the storage modulus variations in terms of h-BN particles, SWCNT coatings, and temperature. The neat fabric/10 wt% h-BN exhibits the highest storage modulus value at room temperature, and the storage modulus, which refers to the load-bearing properties of the composites, is improved by efficient stress transfer between filler and matrix and the stiffening effect of rigid fillers on the matrix [67]. Furthermore, the high surface areas and energy of h-BN particles restrict the molecular movement of the epoxy chains, which improves the storage modulus [68]. The composites, including h-BN particles, have high storage modulus values at room temperature; nonetheless, these values show significant decrement and have lower values at high temperatures, which is

attributed to debonding mechanisms between h-BN and epoxy taking place owing to differential thermal expansion coefficient at high temperatures [57]. On the other hand, the storage modulus values of the composites are degraded by insertion of the SWCNT coated glass fibers in the composite system, and the lowest storage modulus value was obtained at full coated fabric/neat resin design because the rigidity of the composites is reduced by usage of the SWCNT coated fibers. The storage modulus values show sharp decreases in the area, which is named the glass transition region, as seen in Fig. 25a. This decrease takes place due to increasing the molecular mobility and the relaxation reaction in the epoxy chains at high temperatures [66].

The loss factor is the ratio of the storage and loss modulus, as well as named as damping factor. The peak point of the tan delta points out the glass transition temperature of composites, thereby transitioning from a glassy state to a rubbery state. Fig. 25b exhibits the T_g variation and energy dissipation properties of the composites with several designs from variations in positioning on the x-axis and the highness of the curves, respectively. The addition of h-BN particles into epoxy slightly decreases the T_g value compared with neat resin, and the small amount of degradation in the T_g values is attributed to decreasing in the cross-linked density of the epoxy by the addition of the nanomaterials in the system. In addition, the h-BN particles with high surface area interact with the epoxy chains and give an immobilized structure; therefore, this structure does not participate in the curing reaction and reduces the cross-linked density and T_g of the final structure [57]. On the other hand, T_g of hybrid fiber composite systems shows 10 °C enhancement, and hybrid fabric/10 wt% m/h-BN epoxy resin has the highest T_g value of 104.88 °C as seen in Fig. 25b. This enhancement in the T_g confirms the synergistic effect of the h-BN particles and SWCNT coatings on the composites, and this behavior refers to the restriction of the polymer chains mobility due to strong interfacial interaction, between fibers and matrix, and reinforcement effect of the h-BN particles on the resin [68].

The highness of the loss factor gives information about the energy dissipation characteristics of the composites, and neat fabric/10 wt% m/h-BN composite has the highest loss factor. The incorporation of the h-BN particles increases the highness of the loss factor curve, which is due to the low interfacial interaction between h-BN particles and epoxy. In contrast, the usage of the h-BN particles and SWCNT in the composites systems creates consistent structure and decreases the highness of the loss factor, and the lowest loss factor value is attained for hybrid fabric/neat resin. The lowering of the

highness of the loss factor is related to restriction of the epoxy chain mobility and less energy dissipation characteristics of the composites [69][70].

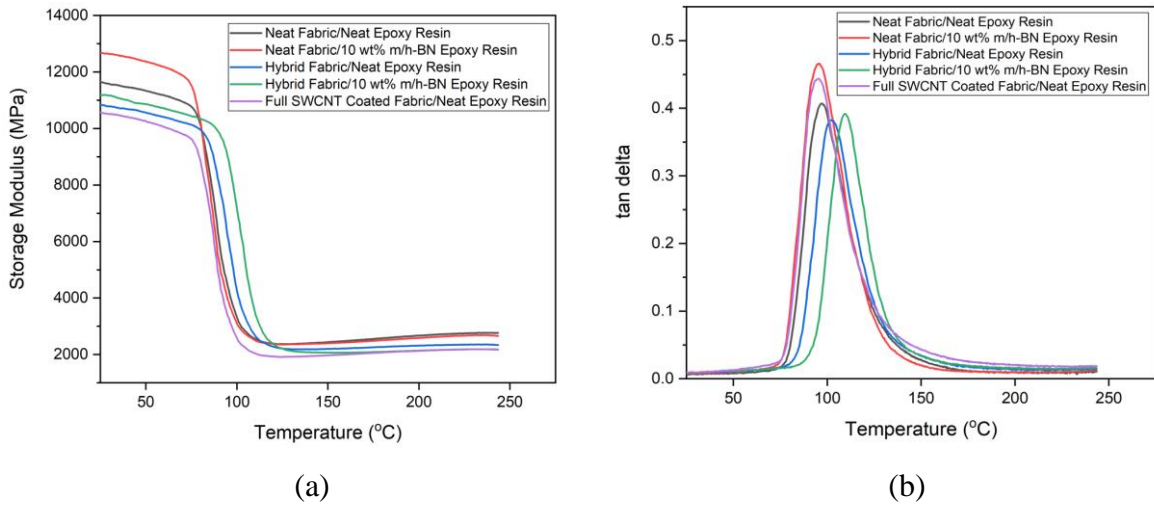


Figure 23. (a) Temperature sweeps of the storage modulus and (b) damping ratio curves of the composite with different designs

3.2.4. Tailored thermal conductivity of composites as a function of h-BN incorporation in resin and SWCNT coating in interface

The composite materials, which consist of components such as fibers, fillers, and matrix, have a lot of interfacial areas, which leads to asymmetrical thermal properties due to phonon scattering in these areas; thus, the thermal conductivity of the composites must be investigated to establish a deep understanding of this anisotropic behavior [71]. Lattice vibration, named phonon, is the primary thermal energy transportation phenomenon in materials [72].

Fig. 26 shows the in-plane and through-thickness thermal conductivity variations of the composites as a function of h-BN and SWCNT concentration. In all designs, in-plane thermal conductivity values are higher than the through-thickness values because the glass fibers have higher thermal conductivity values than epoxy and exhibit anisotropic thermal conductivity properties [73]. In addition, the continuous and stable thermal conductivity pathway is established in the in-plane direction; however, the thermal conductivity pathway is scattered, which reduces the thermal conductivity due to the high number of interfacial areas between fibers and matrix in the through-thickness direction. Furthermore, the moderate thermal conductivity enhancement, which corresponds to 9.23% for hybrid fabric/10 wt% m/h-BN epoxy resin composite, is observed in in-plane directions by the addition of the h-BN particles in epoxy. The thermal conductivity in the

in-plane direction is dependent on the orientation of the fibers, and the addition of micron-sized h-BN in resin does not significantly affect the thermal conductivity. In contrast, h-BN particles significantly improve the thermal conductivity values of composites which is 32% for hybrid fabric/10 wt% m/h-BN in through-thickness directions because the epoxy directly affects the thermal conductivity, and lattice movement decreases the phonon scattering in the through-thickness direction [66][72]. Furthermore, the continuous thermal conductive pathway is established with the incorporation of the high thermal conductive h-BN particles in epoxy, and the h-BN particles start to touch each other at high loading levels, which facilitates heat diffusion [74]. However, thermal resistance can take place when the h-BN particles are agglomerated in a high concentration because the excessive epoxy fills out the spaces among h-BN particles, which increases the thermal resistance in case of formation of agglomerations [75].

There is no physical bonding between the glass fibers in the through-thickness direction; hence, the interfacial regions between epoxy and glass fibers reduce the thermal conductivity by the increment of the phonon scattering [71]. There is no effect of the small amount of SWCNT coating on the thermal conductivity of the composites in the in-plane direction; however, SWCNT coating slightly improves the thermal conductivity, which is 10% for full SWCNT coated fabric/neat epoxy resin in through-thickness direction, as seen in Fig. 26. The SWCNT coating provides an effective bridging effect, which enhances the phonon diffusion for thermal conduction between the matrix and glass fibers and increases the surface roughness and surface area of the fibers, thereby the specific surface energy of the fibers and carrying of the energy is enhanced between matrix and glass fibers [72]. Besides, the thermal conductivity of the composites is enhanced through the formation of several conductive branches, and the surface energy gap between glass fiber and the epoxy matrix is reduced via surface coating of the fibers created by SWCNT [76].

Table 10. The thermal conductivity values and their improvements of the glass fiber reinforced composites with different designs in in-plane and through-thickness directions as a function of h-BN and SWCNT in resin and interfaces

Samples	Density of Composites (g/cm ³)	In-Plane Thermal	Improvement (%)	Through-Thickness Thermal	Improvement (%)

		Conductivity (W/m.K)		Conductivity (W/m.K)	
Neat Fabric/Neat Epoxy Resin	2.05	0.65	—	0.50	—
Neat Fabric/10.0 wt% m/h-BN Epoxy Resin	2.06	0.71	9.23	0.61	22.00
Hybrid Fabric/Neat Epoxy Resin	2.03	0.61	- 6.15	0.54	8.00
Hybrid Fabric/10.0 wt% m/h-BN Epoxy Resin	2.06	0.71	9.23	0.66	32.00
Full SWCNT Coated Fabric/Neat Epoxy Resin	2.03	0.65	—	0.55	10.00

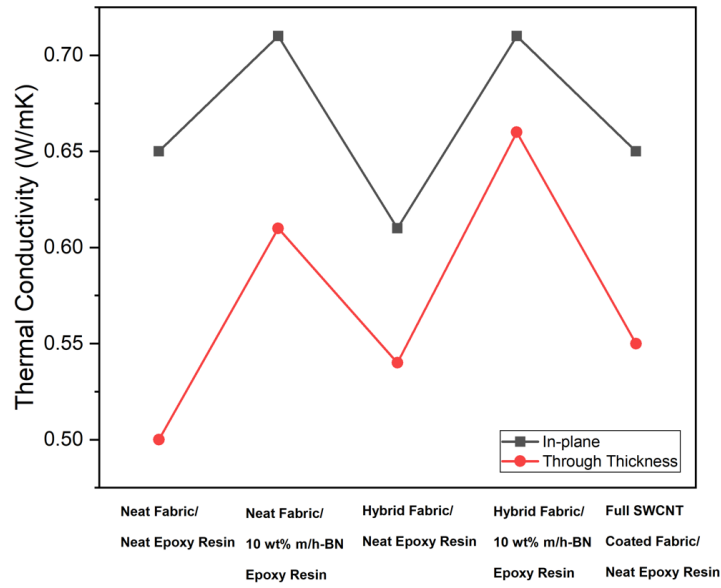


Figure 24. Comparison of the in-plane and through-thickness thermal conductivity values of the composites with different designs as a function of h-BN and SWCNT particles in resin and interfaces

3.3 Conclusion

The pre-dispersion method is utilized for the dispersion of h-BN particles in epoxy to attain a homogeneous and highly stable h-BN/epoxy mixture. The heat and load transfers are facilitated by the incorporation of the h-BN; thereby, the thermal and mechanical properties of composites exhibit enhancement. Furthermore, dip coating, which is a quick, up-scalable, and efficient method, is employed for SWCNT deposition onto glass fibers to restrain mismatch between epoxy and glass fibers. The DMA analysis shows no deterioration of the thermomechanical properties of h-BN reinforced epoxy composites, and the thermal consistency is maintained even at high temperatures. In addition, the Raman spectroscopy analysis verifies that there is no adverse effect of the deposition of the h-BN particles on the chemical and structural properties of glass fibers by the dip-coating method.

10 wt% h-BN particles were selected due to their obtaining high thermal properties with promising mechanical performance as investigated in the previous section, and the effect of h-BN particles as primary resin modifiers on glass fiber composites is investigated. A highly stable and homogeneous h-BN/epoxy mixture was prepared by pre-dispersion method to inhibit aggregation of particles by using probe sonication; subsequently, the degassed h-BN/epoxy mixture was infused into glass fiber combinations to fabricate glass

fiber reinforced epoxy composites by VARTM. The incorporation of h-BN particles in composite designs as a resin modifier gives notable enhancement in thermal and mechanical properties. Moreover, h-BN particles and SWCNT as resin and interfacial modifiers exhibit a synergistic effect; thereby, the thermal conductivity and impact strength improve by 32% and 42% with respect to neat reference composite, respectively.

CHAPTER 4. CONCLUSION

This study was carried out in two major sections, and the findings for each section can be summarized as follow:

i. The effect of particle size and loading ratio of hexagonal boron nitride (h-BN) particles on the thermal management and mechanical performance of epoxy composites

Micron- and nano-sized h-BN particles are incorporated in epoxy to fabricate high thermal conductive composites in a wide loading ratio to evaluate the effects of particle size and weight ratio on thermal and mechanical performance of glass fiber reinforced composites. Firstly, the loading ratio was investigated as the primary parameter, and the micron-sized h-BN particles with a weight ratio from 0.5 wt% to 20 wt% were incorporated in epoxy by the pre-dispersion method. The thermal and mechanical performances of the epoxy were improved by homogeneous and stable dispersion of the micron-sized h-BN particles resulting in effective heat diffusion and load transfer. In the second approach, the effect of the particle size on the properties of the epoxy was investigated by dispersion of the nano-sized h-BN particles in the same loading ratios in epoxy. The physical and chemical characterization techniques were employed to reveal the synergetic effects of size and loading ratio of h-BN particles. The increment of the particle size and loading ratio positively affected the thermal and mechanical properties of epoxy. In the micron-sized h-BN reinforced epoxy, noticeable enhancements were observed in thermal conductivity in in-plane and through-thickness directions by 107% and 112%, respectively, with the 20 wt% loading level of h-BN, and outstanding improvement in tensile modulus by 41% as well as flexural modulus by 42% by the addition of 10 wt% h-BN. To conclude, the incorporation of different-sized particles in resin establishes a deep understanding of the mechanism behind thermal and mechanical performance enhancements of thermoset polymers to attain a place in the aerospace industry.

ii. The synergistic effect of carbon nanomaterial coated glass fibers on the performance of epoxy composites having h-BN particles

Four different designs are evaluated to fabricate multi-scale epoxy composites in which micron-sized h-BN particles were dispersed into resin and nano-sized SWCNT were coated on the surface of glass fibers used as primary reinforcement. In the first design,

the micron-sized h-BN particles were incorporated into the resin by the pre-dispersion method, which provides a homogeneous and highly stable mixture. The efficient heat and load transfer pathway has improved thermal and mechanical properties of glass fiber reinforced composites due to the homogeneous dispersion of h-BN particles in resin. In the second design, the glass fibers were coated by SWCNT by dip coating to inhibit a thermal mismatch between glass fibers and epoxy. In the third design, the hybrid system was developed utilizing the neat and SWCNT coated glass fibers to observe the gradual enhancement in the thermal and mechanical properties of the composites. In the last design, h-BN reinforced epoxy was infused into the hybrid fiber combination to produce the multi-scale composite system. Several physical and chemical characterization methods were employed to evaluate the effects of resin and interface modifiers, and the remarkable thermal and thermomechanical performance was observed due to the synergistic effects of the h-BN and SWCNT particles. The utilizing of h-BN particles for all developed composites enhances the thermal performance in in-plane and through-thickness directions, and the hybrid systems with h-BN particles exhibit outstanding thermal performance in the through-thickness direction by 32%. To conclude, these kinds of composite structures reinforced by different sized structures together with main reinforcement like glass fibers open up a way to design lightweight structures with high toughness and controlling the heat and load transfer in structural applications.

REFERENCES

- [1] E. Petrie, *Epoxy Adhesive Formulations*. Mc Graw Hill, 2005.
- [2] J. Hou *et al.*, “Preparation and characterization of surface modified boron nitride epoxy composites with enhanced thermal conductivity,” 2014, doi: 10.1039/c4ra07394k.
- [3] S. Han *et al.*, “Mechanical, toughness and thermal properties of 2D material-reinforced epoxy composites,” *Polymer (Guildf)*, vol. 184, p. 121884, Dec. 2019, doi: 10.1016/J.POLYMER.2019.121884.
- [4] L. Huang *et al.*, “Spherical and flake-like BN filled epoxy composites: morphological effect on the thermal conductivity, thermo-mechanical and dielectric properties,” *Journal of Materials Science: Materials in Electronics*, vol. 26, no. 6, pp. 3564–3572, Jun. 2015, doi: 10.1007/s10854-015-2870-1.
- [5] J. M. Hutchinson and S. Moradi, “Materials Thermal Conductivity and Cure Kinetics of Epoxy-Boron Nitride Composites-A Review”, doi: 10.3390/ma13163634.
- [6] Z. Zheng, M. C. Cox, and B. Li, “Surface modification of hexagonal boron nitride nanomaterials: a review,” *Journal of Materials Science*, vol. 53, no. 1. Springer New York LLC, pp. 66–99, Jan. 01, 2018. doi: 10.1007/s10853-017-1472-0.
- [7] C. Yuan *et al.*, “Modulating the thermal conductivity in hexagonal boron nitride via controlled boron isotope concentration,” *Communications Physics*, vol. 2, no. 1, Dec. 2019, doi: 10.1038/s42005-019-0145-5.
- [8] S. Zhang *et al.*, “Thermal properties of amino-functionalized multi-walled carbon nanotubes reinforced epoxy-based transducers embedded in concrete,” *Cement and Concrete Composites*, vol. 127, p. 104411, Mar. 2022, doi: 10.1016/J.CEMCONCOMP.2022.104411.
- [9] R. Wang *et al.*, “Epoxy nanocomposites with high thermal conductivity and low loss factor: Realize 3D thermal conductivity network at low content through core-shell structure and micro-nano technology,” *Polymer Testing*, vol. 89, p. 106574, Sep. 2020, doi: 10.1016/J.POLYMERTESTING.2020.106574.

- [10] J. Wang, Y. Li, X. Liu, C. Shen, H. Zhang, and K. Xiong, "Recent active thermal management technologies for the development of energy-optimized aerospace vehicles in China," *Chinese Journal of Aeronautics*, vol. 34, no. 2, pp. 1–27, Feb. 2021, doi: 10.1016/J.CJA.2020.06.021.
- [11] R. Wang, C. Xie, S. Luo, H. Xu, B. Gou, and L. Zeng, "Preparation and properties of MWCNTs-BNNSs/epoxy composites with high thermal conductivity and low dielectric loss," *Materials Today Communications*, vol. 24, p. 100985, Sep. 2020, doi: 10.1016/J.MTCOMM.2020.100985.
- [12] L. Liu, D. Xiang, and L. Wu, "Improved thermal conductivity of ceramic-epoxy composites by constructing vertically aligned nanoflower-like AlN network," *Ceramics International*, vol. 48, no. 8, pp. 10438–10446, Apr. 2022, doi: 10.1016/J.CERAMINT.2021.12.252.
- [13] N. Aliyeva, H. S. Sas, and B. Saner Okan, "Recent developments on the overmolding process for the fabrication of thermoset and thermoplastic composites by the integration of nano/micron-scale reinforcements," *Composites Part A: Applied Science and Manufacturing*, vol. 149, p. 106525, Oct. 2021, doi: 10.1016/J.COMPOSITESA.2021.106525.
- [14] Y. Hu *et al.*, "Novel micro-nano epoxy composites for electronic packaging application: Balance of thermal conductivity and processability," *Composites Science and Technology*, vol. 209, p. 108760, Jun. 2021, doi: 10.1016/J.COMPSCITECH.2021.108760.
- [15] L. Ma, G. Song, X. C. Zhang, S. Zhou, Y. Liu, and L. Zhang, "Attaching SiO₂ nanoparticles to GO sheets via amino-terminated hyperbranched polymer for epoxy composites: Extraordinary improvement in thermal and mechanical properties," *European Polymer Journal*, vol. 157, p. 110677, Aug. 2021, doi: 10.1016/J.EURPOLYMJ.2021.110677.
- [16] R. Kumar, "Functionalities of ZnO reinforced thermoplastics composite materials: A state of the art review," *Materials Today: Proceedings*, vol. 51, pp. 972–976, Jan. 2022, doi: 10.1016/J.MATPR.2021.07.020.
- [17] V. Sharma, M. Lal Meena, A. Kumar Chaudhary, and M. Kumar, "Cenosphere powder filled basalt fiber reinforced epoxy composite: Physical, mechanical, and

- thermal conductivity analysis,” *Materials Today: Proceedings*, vol. 44, pp. 4984–4989, Jan. 2021, doi: 10.1016/J.MATPR.2020.12.938.
- [18] J. Hao *et al.*, “Fabrication of long bamboo fiber-reinforced thermoplastic composite by extrusion and improvement of its properties,” *Industrial Crops and Products*, vol. 173, p. 114120, Dec. 2021, doi: 10.1016/J.INDCROP.2021.114120.
- [19] C. Schilde, M. Schlömann, A. Overbeck, S. Linke, and A. Kwade, “Thermal, mechanical and electrical properties of highly loaded CNT-epoxy composites – A model for the electric conductivity,” *Composites Science and Technology*, vol. 117, pp. 183–190, Sep. 2015, doi: 10.1016/J.COMPSCITECH.2015.06.013.
- [20] X. Yang, Z. Wang, M. Xu, R. Zhao, and X. Liu, “Dramatic mechanical and thermal increments of thermoplastic composites by multi-scale synergetic reinforcement: Carbon fiber and graphene nanoplatelet,” *Materials & Design*, vol. 44, pp. 74–80, Feb. 2013, doi: 10.1016/J.MATDES.2012.07.051.
- [21] J. Gu, Q. Zhang, J. Dang, and C. Xie, “Thermal conductivity epoxy resin composites filled with boron nitride,” 2011, doi: 10.1002/pat.2063.
- [22] Y. Tang *et al.*, “Materials Temperature Effects on the Dielectric Properties and Breakdown Performance of h-BN/Epoxy Composites”, doi: 10.3390/ma12244112.
- [23] H. Yan, Y. Tang, J. Su, and X. Yang, “Enhanced thermal-mechanical properties of polymer composites with hybrid boron nitride nanofillers”, doi: 10.1007/s00339-013-8149-6.
- [24] J. Joy, E. George, S. Thomas, and S. Anas, “Effect of filler loading on polymer chain confinement and thermomechanical properties of epoxy/boron nitride (h-BN) nanocomposites,” *This journal is Cite this: New J. Chem*, vol. 44, p. 4494, 2020, doi: 10.1039/c9nj05834f.
- [25] W. Li, D. He, and J. Bai, “The influence of nano/micro hybrid structure on the mechanical and self-sensing properties of carbon nanotube-microparticle reinforced epoxy matrix composite,” *Composites Part A: Applied Science and Manufacturing*, vol. 54, pp. 28–36, Nov. 2013, doi: 10.1016/J.COMPOSITESA.2013.07.002.

- [26] W. Chen *et al.*, “Controllable synthesis of boron nitride submicron tubes and their excellent mechanical property and thermal conductivity applied in the epoxy resin polymer composites,” *Composites Part A: Applied Science and Manufacturing*, vol. 154, p. 106783, Mar. 2022, doi: 10.1016/J.COMPOSITESA.2021.106783.
- [27] M. Saha *et al.*, “Composite Interfaces Effect of non-ionic surfactant assisted modification of hexagonal boron nitride nanoplatelets on the mechanical and thermal properties of epoxy nanocomposites,” 2015, doi: 10.1080/09276440.2015.1056688.
- [28] K. Wattanakul, H. Manuspiya, and N. Yanumet, “The adsorption of cationic surfactants on BN surface: Its effects on the thermal conductivity and mechanical properties of BN-epoxy composite,” *Colloids and Surfaces A: Physicochemical and Engineering Aspects*, vol. 369, no. 1–3, pp. 203–210, Oct. 2010, doi: 10.1016/J.COLSURFA.2010.08.021.
- [29] W. Jin, W. Zhang, Y. Gao, G. Liang, A. Gu, and L. Yuan, “Surface functionalization of hexagonal boron nitride and its effect on the structure and performance of composites,” *Applied Surface Science*, vol. 270, pp. 561–571, Apr. 2013, doi: 10.1016/J.APSUSC.2013.01.086.
- [30] S. Zhang *et al.*, “Synthesis of pyridine-containing diamine and properties of its polyimides and polyimide/hexagonal boron nitride composite films,” *Composites Science and Technology*, vol. 152, pp. 165–172, Nov. 2017, doi: 10.1016/J.COMPSCITECH.2017.09.026.
- [31] L. Saravanan, “Polymeric Materials and Their Components for Biomedical Applications,” in *Materials Development and Processing for Biomedical Applications*, CRC Press, 2022, pp. 91–105.
- [32] J. Song, Z. Dai, J. Li, X. Tong, and H. Zhao, “Polydopamine-decorated boron nitride as nano-reinforcing fillers for epoxy resin with enhanced thermomechanical and tribological properties,” *Mater. Res. Express*, vol. 5, p. 75029, 2018, doi: 10.1088/2053-1591/aab529.
- [33] X. Wen *et al.*, “Constructing Novel Fiber Reinforced Plastic (FRP) Composites through a Biomimetic Approach: Connecting Glass Fiber with Nanosized Boron

- Nitride by Polydopamine Coating,” *Journal of Nanomaterials*, vol. 2013, 2013, doi: 10.1155/2013/470583.
- [34] Y. Wang, J. Wu, T. Han, and Y. Yin, *Enhanced Thermal Conductive Boron Nitride/ Silicon Carbide/ Silicone Elastomer with Nonlinear Conductive Characteristic and Partial Discharge Resistance; Enhanced Thermal Conductive Boron Nitride/ Silicon Carbide/ Silicone Elastomer with Nonlinear Conductive Characteristic and Partial Discharge Resistance*. 2019. doi: 10.1109/CEIDP47102.2019.9009730.
- [35] K. C. Yung, J. Wang, and T. M. Yue, “Thermal Management for Boron Nitride Filled Metal Core Printed Circuit Board”, doi: 10.1177/0021998308096326.
- [36] J. Yu, X. Huang, C. Wu, X. Wu, G. Wang, and P. Jiang, “Interfacial modification of boron nitride nanoplatelets for epoxy composites with improved thermal properties,” *Polymer (Guildf)*, vol. 53, no. 2, pp. 471–480, Jan. 2012, doi: 10.1016/J.POLYMER.2011.12.040.
- [37] H. Y. Ng, X. Lu, and S. K. Lau, “Thermal Conductivity of Boron Nitride-Filled Thermoplastics: Effect of Filler Characteristics and Composite Processing Conditions,” 2005, doi: 10.1002/pc.20151.
- [38] H. Yetgin, S. Veziroglu, O. C. Aktas, and T. Yalçinkaya, “Enhancing thermal conductivity of epoxy with a binary filler system of h-BN platelets and Al₂O₃ nanoparticles,” *International Journal of Adhesion and Adhesives*, vol. 98, p. 102540, Apr. 2020, doi: 10.1016/J.IJADHADH.2019.102540.
- [39] H. Chen *et al.*, “Thermal conductivity of polymer-based composites: Fundamentals and applications,” *Progress in Polymer Science*, vol. 59, pp. 41–85, Aug. 2016, doi: 10.1016/J.PROGPOLYMSCI.2016.03.001.
- [40] W.-Y. Zhou, S.-H. Qi, H.-Z. Zhao, and N.-L. Liu, “Thermally Conductive Silicone Rubber Reinforced With Boron Nitride Particle,” 2007, doi: 10.1002/pc.20296.
- [41] K. Wattanakul, H. Manuspiya, and N. Yanumet, “Effective Surface Treatments for Enhancing the Thermal Conductivity of BN-Filled Epoxy Composite,” *J Appl Polym Sci*, vol. 119, pp. 3234–3243, 2010, doi: 10.1002/app.32889.

- [42] J. Seyyed, M. Zanjani, B. S. Okan, B. Yusuf, Z. Menciloglu, and M. Yildiz, “Nano-engineered design and manufacturing of high-performance epoxy matrix composites with carbon fiber/selectively integrated graphene as multi-scale reinforcements †,” 2016, doi: 10.1039/c5ra23665g.
- [43] A. Jorio and R. Saito, “Raman spectroscopy for carbon nanotube applications,” *Journal of Applied Physics*, vol. 129, no. 2, Jan. 2021, doi: 10.1063/5.0030809.
- [44] F. Azimpour-Shishevan, H. Akbulut, and M. A. Mohtadi-Bonab, “Synergetic effects of carbon nanotube and graphene addition on thermo-mechanical properties and vibrational behavior of twill carbon fiber reinforced polymer composites,” *Polymer Testing*, vol. 90, p. 106745, Oct. 2020, doi: 10.1016/J.POLYMERTESTING.2020.106745.
- [45] S. C. Tjong, “Polymer nanocomposite bipolar plates reinforced with carbon nanotubes and graphite nanosheets,” *Energy and Environmental Science*, vol. 4, no. 3, pp. 605–626, 2011, doi: 10.1039/c0ee00689k.
- [46] M. Megahed, A. Fathy, D. Morsy, and F. Shehata, “Mechanical Performance of glass/epoxy composites enhanced by micro- and nanosized aluminum particles,” *Journal of Industrial Textiles*, vol. 51, no. 1, pp. 68–92, 2021, doi: 10.1177/1528083719874479.
- [47] K. Gültekin, | Gediz U Guz, and | Adnan Özel, “Improvements of the structural, thermal, and mechanical properties of structural adhesive with functionalized boron nitride nanoparticles,” 2021, doi: 10.1002/app.50491.
- [48] M. Tehrani, A. Y. Boroujeni, T. B. Hartman, T. P. Haugh, S. W. Case, and M. S. Al-Haik, “Mechanical characterization and impact damage assessment of a woven carbon fiber reinforced carbon nanotube-epoxy composite,” *Composites Science and Technology*, vol. 75, pp. 42–48, Feb. 2013, doi: 10.1016/j.compscitech.2012.12.005.
- [49] X. Zheng and C. W. Park, “Thermal and mechanical properties of carbon fiber-reinforced resin composites with copper/boron nitride coating,” *Composite Structures*, vol. 220, pp. 494–501, Jul. 2019, doi: 10.1016/j.compstruct.2019.03.089.

- [50] K. K. Panchagnula and P. Kuppan, "Improvement in the mechanical properties of neat GFRPs with multi-walled CNTs," *Journal of Materials Research and Technology*, vol. 8, no. 1, pp. 366–376, Jan. 2019, doi: 10.1016/j.jmrt.2018.02.009.
- [51] K. Li, R. Zhao, J. Xia, and G. L. Zhao, "Reinforcing Microwave Absorption Multiwalled Carbon Nanotube–Epoxy Composites Using Glass Fibers for Multifunctional Applications," *Advanced Engineering Materials*, vol. 22, no. 3, Mar. 2020, doi: 10.1002/adem.201900780.
- [52] S. Saadatyar, M. H. Beheshty, and R. Sahraeian, "Mechanical properties of multiwall carbon nanotubes/unidirectional carbon fiber-reinforced epoxy hybrid nanocomposites in transverse and longitudinal fiber directions," *Polymers and Polymer Composites*, vol. 29, no. 9_suppl, pp. S74–S84, Nov. 2021, doi: 10.1177/0967391120986516.
- [53] N. R. Abdelal, M. H. Al-Saleh, and M. R. Irshidat, "Utilizing Vacuum Bagging Process to Prepare Carbon Fiber/CNT-Modified-epoxy Composites with Improved Mechanical Properties," *Polymer - Plastics Technology and Engineering*, vol. 57, no. 3, pp. 175–184, Feb. 2018, doi: 10.1080/03602559.2017.1315644.
- [54] T. Subhani, B. Shaukat, N. Ali, and A. A. Khurram, "Toward improved mechanical performance of multiscale carbon fiber and carbon nanotube epoxy composites," *Polymer Composites*, vol. 38, no. 8, pp. 1519–1528, Aug. 2017, doi: 10.1002/pc.23719.
- [55] W. A. D. Wan Dalina, M. Mariatti, R. Ramlee, Z. A. M. Ishak, and A. R. Mohamed, "Comparison on the properties of glass fiber/MWCNT/epoxy and carbon fiber/MWCNT/epoxy composites," in *Advanced Materials Research*, 2014, vol. 858, pp. 32–39. doi: 10.4028/www.scientific.net/AMR.858.32.
- [56] M. Sánchez, M. Campo, A. Jiménez-Suárez, and A. Ureña, "Effect of the carbon nanotube functionalization on flexural properties of multiscale carbon fiber/epoxy composites manufactured by VARIM," *Composites Part B: Engineering*, vol. 45, no. 1, pp. 1613–1619, Feb. 2013, doi: 10.1016/j.compositesb.2012.09.063.
- [57] A. O. Fulmali, B. Sen, B. A. Nayak, and R. K. Prusty, "Effect of repeated hydrothermal cycling on the durability of glass fiber/epoxy composites with and

- without carbon nanotube reinforcement,” *Polymer Composites*, vol. 42, no. 11, pp. 6160–6172, Nov. 2021, doi: 10.1002/pc.26293.
- [58] F. H. Gojny, M. H. G. Wichmann, B. Fiedler, and K. Schulte, “Influence of different carbon nanotubes on the mechanical properties of epoxy matrix composites - A comparative study,” *Composites Science and Technology*, vol. 65, no. 15-16 SPEC. ISS., pp. 2300–2313, Dec. 2005, doi: 10.1016/j.compscitech.2005.04.021.
- [59] N. M. Zulfli, A. A. Bakar, and W. S. Chow, “Mechanical and water absorption behaviors of carbon nanotube reinforced epoxy/glass fiber laminates,” *Journal of Reinforced Plastics and Composites*, vol. 32, no. 22, pp. 1715–1721, Nov. 2013, doi: 10.1177/0731684413501926.
- [60] Y. Wu, D. Dhamodharan, Z. Wang, R. Wang, and L. Wu, “Effect of electrophoretic deposition followed by solution pre-impregnated surface modified carbon fiber-carbon nanotubes on the mechanical properties of carbon fiber reinforced polycarbonate composites,” *Composites Part B: Engineering*, vol. 195, Aug. 2020, doi: 10.1016/j.compositesb.2020.108093.
- [61] G. Wu *et al.*, “Interface enhancement of carbon fiber reinforced methylphenylsilicone resin composites modified with silanized carbon nanotubes,” *Materials and Design*, vol. 89, pp. 1343–1349, Jan. 2016, doi: 10.1016/j.matdes.2015.10.016.
- [62] M. Q. Tran, K. K. C. Ho, G. Kalinka, M. S. P. Shaffer, and A. Bismarck, “Carbon fibre reinforced poly(vinylidene fluoride): Impact of matrix modification on fibre/polymer adhesion,” *Composites Science and Technology*, vol. 68, no. 7–8, pp. 1766–1776, Jun. 2008, doi: 10.1016/j.compscitech.2008.02.021.
- [63] G. Wu, L. Ma, Y. Wang, L. Liu, and Y. Huang, “Improvements in interfacial and heat-resistant properties of carbon fiber/methylphenylsilicone resins composites by incorporating silica-coated multi-walled carbon nanotubes,” *Journal of Adhesion Science and Technology*, vol. 30, no. 2, pp. 117–130, Jan. 2016, doi: 10.1080/01694243.2015.1092370.

- [64] M. Rahmat *et al.*, “Enhanced shear performance of hybrid glass fiber-epoxy laminates modified with boron nitride nanotubes,” *ACS Applied Nano Materials*, vol. 1, no. 6, pp. 2709–2717, Jun. 2018, doi: 10.1021/acsanm.8b00413.
- [65] T. Peijs, F. Inam, D. W. Y. Wong, and M. Kuwata, “Multiscale hybrid micro-nanocomposites based on carbon nanotubes and carbon fibers,” *Journal of Nanomaterials*, vol. 2010, 2010, doi: 10.1155/2010/453420.
- [66] X. Wen *et al.*, “Constructing novel fiber reinforced plastic (FRP) composites through a biomimetic approach: Connecting glass fiber with nanosized boron nitride by polydopamine coating,” *Journal of Nanomaterials*, vol. 2013, 2013, doi: 10.1155/2013/470583.
- [67] P. v Joseph, G. Mathew, K. Joseph, G. Groeninckx, and S. Thomas, “Dynamic mechanical properties of short sisal @bre reinforced polypropylene composites.” [Online]. Available: www.elsevier.com/locate/compositesa
- [68] P. Wang *et al.*, “Improvement of impact-resistant property of glass fiber-reinforced composites by carbon nanotube-modified epoxy and pre-stretched fiber fabrics,” *Journal of Materials Science*, vol. 50, no. 18, pp. 5978–5992, Sep. 2015, doi: 10.1007/s10853-015-9145-3.
- [69] J. A. Rojas, L. F. de Paula Santos, E. C. Botelho, B. Ribeiro, and M. C. Rezende, “Morphological, mechanical, and electromagnetic interference shielding effectiveness characteristics of glass fiber/epoxy resin/MWCNT buckypaper composites,” *Journal of Applied Polymer Science*, vol. 138, no. 25, Jul. 2021, doi: 10.1002/app.50589.
- [70] J. Jyoti, B. P. Singh, A. K. Arya, and S. R. Dhakate, “Dynamic mechanical properties of multiwall carbon nanotube reinforced ABS composites and their correlation with entanglement density, adhesion, reinforcement and C factor,” *RSC Advances*, vol. 6, no. 5, pp. 3997–4006, 2016, doi: 10.1039/c5ra25561a.
- [71] P. Venkataramanaiah, R. Aradhya, and S. Rajan J, “Investigations on the effect of hybrid carbon fillers on the thermal conductivity of glass epoxy composites,” *Polymer Composites*, vol. 42, no. 2, pp. 618–633, Feb. 2021, doi: 10.1002/pc.25852.

- [72] A. Badakhsh, W. Han, S. C. Jung, K. H. An, and B. J. Kim, "Preparation of boron nitride-coated carbon fibers and synergistic improvement of thermal conductivity in their polypropylene-matrix composites," *Polymers (Basel)*, vol. 11, no. 12, Dec. 2019, doi: 10.3390/polym11122009.
- [73] X. Zheng, S. Kim, and C. W. Park, "Enhancement of thermal conductivity of carbon fiber-reinforced polymer composite with copper and boron nitride particles," *Composites Part A: Applied Science and Manufacturing*, vol. 121, pp. 449–456, Jun. 2019, doi: 10.1016/j.compositesa.2019.03.030.
- [74] Z. Meng, Z. Dai, K. Chen, and S. Wang, "Investigation on preparation, thermal, and mechanical properties of carbon fiber decorated with hexagonal boron nitride/silicone rubber composites for battery thermal management," *International Journal of Energy Research*, vol. 45, no. 3, pp. 4396–4409, Mar. 2021, doi: 10.1002/er.6110.
- [75] F. An, X. Li, P. Min, H. Li, Z. Dai, and Z. Z. Yu, "Highly anisotropic graphene/boron nitride hybrid aerogels with long-range ordered architecture and moderate density for highly thermally conductive composites," *Carbon N Y*, vol. 126, pp. 119–127, Jan. 2018, doi: 10.1016/j.carbon.2017.10.011.
- [76] J. Li, Z. Wu, C. Huang, and L. Li, "Multiscale carbon nanotube-woven glass fiber reinforced cyanate ester/epoxy composites for enhanced mechanical and thermal properties," *Composites Science and Technology*, vol. 104, pp. 81–88, Dec. 2014, doi: 10.1016/j.compscitech.2014.09.007.